

CMFGEN

History, ingredients and how to cook it right

Prepared by **Olga Maryeva** (ASU)

for “Stellar Winds and Outflows” Summer School
Harrachov, 3-15 September, 2023



Astronomický
ústav
AV ČR



WOLFRAM

Transfer Equation

$$\left(\frac{1}{c} \frac{\partial}{\partial t} + \frac{\partial}{\partial s} \right) I(\mathbf{r}, \mathbf{n}, \nu, t) = \eta(\mathbf{r}, \mathbf{n}, \nu, t) - \chi(\mathbf{r}, \mathbf{n}, \nu, t) I(\mathbf{r}, \mathbf{n}, \nu, t)$$

transfer equation in general form

Transfer Equation

$$\left(\frac{1}{c} \frac{\partial}{\partial t} + \frac{\partial}{\partial s} \right) I(\mathbf{r}, \mathbf{n}, \nu, t) = \eta(\mathbf{r}, \mathbf{n}, \nu, t) - \chi(\mathbf{r}, \mathbf{n}, \nu, t) I(\mathbf{r}, \mathbf{n}, \nu, t)$$

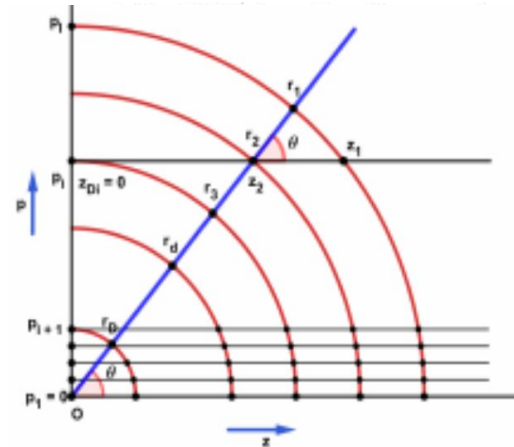
transfer equation in general form

$$\left(\mu \frac{\partial}{\partial r} + \frac{1 - \mu^2}{r} \frac{\partial}{\partial \mu} \right) I(r, \mu, \nu) = \eta(r, \mu, \nu) - \chi(r, \nu) I(r, \mu, \nu)$$

*transfer equation in case of static
spherically symmetric atmosphere*

Transfer Equation

Despite this increase in *mathematical* complexity, the basic *conceptual* and *physical advantages* described above are so substantial that the motivation to use a comoving-frame formulation is compelling. By assuming complete redistribution over a rectangular profile in the comoving frame, and considering all radiation to flow at the same angle to the radius vector, Chandrasekhar (1945) was able to solve these partial differential equations in the case of plane geometry and a linear velocity law. Although his approach was generalized slightly by Abhyankar (1964*a, b*, 1965), the treatment of line formation problems in the comoving fluid frame has not advanced significantly until recently. Simonneau (1973) developed an integral equation method (in planar geometry) that uses comoving coordinates; but in addition to its restriction to velocity laws that are linear in optical depth, it is apparently unstable at large velocities. An additional problem associated with any scheme based on the fluid-frame equations is that a separate calculation is necessary to obtain the emergent radiation field in the frame of a stationary observer. For extended spherical atmospheres this is a nontrivial problem.



Comoving Frame

The Comoving Frame system is more convenient to use for several reasons:

- Absorption and emission coefficients do not depend on angles.
- When solving problems taking into account partial redistribution, you can use the standard redistribution functions.
- When calculating the integrals describing scattering, it suffices to consider only such a frequency band that would completely cover the absorption profile in the line.
- The quadrature formula for the angle can be chosen based only on from what is the angular distribution of radiation.
- Gas dynamic calculations for spherically symmetric flows can be performed with high accuracy in Lagrangian coordinate system (i.e., in the comoving system).

Transfer Equation

$$\left\{ \frac{1}{c} \frac{\partial}{\partial t_0} + \left(\mu_0 + \frac{v}{c} \right) \frac{\partial}{\partial r_0} + \frac{1 - \mu_0^2}{r_0} \left[1 + \frac{\mu_0 v}{c} \left(1 - \frac{d \ln v}{d \ln r_0} \right) \right] \frac{\partial}{\partial \mu_0} - \right. \\ \left. - \frac{\nu_0 v}{c r_0} \left[1 - \mu_0^2 \left(1 - \frac{d \ln v}{d \ln r_0} \right) \right] \frac{\partial}{\partial \nu_0} + \right. \\ \left. + \frac{3v}{c r_0} \left[1 - \mu_0^2 \left(1 - \frac{d \ln v}{d \ln r_0} \right) \right] \right\} \times \\ \times I^0(r_0, \mu_0, \nu_0, t_0) = \eta^0(\nu_0) - \chi^0(\nu_0) I(r_0, \mu_0, \nu_0, t_0)$$

Transport equation in comoving frame with spherical geometry

Transfer Equation

$$\begin{aligned} & \mu_0 \frac{\partial I^0(r, \mu_0, \nu_0)}{\partial r} + \frac{1 - \mu_0^2}{r} \frac{\partial I^0(r, \mu_0, \nu_0)}{\partial \mu_0} - \\ & - \frac{\nu_0 v}{cr} \left(1 - \mu_0^2 + \mu_0^2 \frac{d \ln(v)}{d \ln(r)} \right) \frac{\partial I^0(r, \mu_0, \nu_0)}{\partial \nu_0} = \\ & = \eta^0(r, \mu_0, \nu_0) - \chi^0(r, \nu_0) I^0(r, \mu_0, \nu_0) \end{aligned}$$

simplified transport equation in comoving frame with spherical geometry

Transfer Equation

THE ASTROPHYSICAL JOURNAL, 202:465-489, 1975 December 1
© 1975. The American Astronomical Society. All rights reserved. Printed in U.S.A.

Mihalas et al. 1975, 1976

SOLUTION OF THE COMOVING-FRAME EQUATION OF TRANSFER IN SPHERICALLY SYMMETRIC FLOWS. I. COMPUTATIONAL METHOD FOR EQUIVALENT-TWO-LEVEL-ATOM SOURCE FUNCTIONS

DIMITRI MIHALAS

High Altitude Observatory, National Center for Atmospheric Research*

AND

P. B. KUNASZ AND D. G. HUMMER†

Joint Institute for Laboratory Astrophysics, University of Colorado and National Bureau of Standards,
Boulder

Received 1975 March 19; revised 1975 June 2

ABSTRACT

The equation of radiative transfer in the comoving frame makes possible an economical solution of the line formation problem in spherical atmospheres expanding with arbitrarily large velocities. A stable differencing scheme and a frequency-by-frequency elimination procedure have been developed to solve the partial differential equations that describe the radiation field in the comoving frame. Numerical results were obtained for a large number of illustrative models involving line formation by two-level atoms, electron scattering, and continuous absorption. Selected results that simulate situations in the stellar winds of hot stars and similar objects are discussed. In addition to P Cygni and other very broad profiles, extreme center-to-limb variations are obtained that show both limb darkening and limb brightening. For very high velocity flows with very weak or nonexistent continuum and electron-scattering opacities, the flux profiles are very nearly symmetric about the laboratory wavelength and have shapes reminiscent of those observed in the nuclei of Seyfert galaxies. Comparisons are presented between the results of Sobolev-type escape probability calculations and those obtained here. The force of radiation on the gas is examined in a number of situations; the mechanism mentioned by Noerdlinger and Rybicki for the disruption of radiatively driven envelopes in planar geometries is shown to become inoperative for even slightly extended spherical systems.

Subject headings: atmospheres, stellar — atomic and molecular processes — line formation — radiative transfer

predecessor of CMFGEN

Since middle of 80-s **Desmond John Hillier** was extensively developing a code for solving the radiative transfer equation for objects with spherically extended outflows using either the **Sobolev approximation** or the **full solution of the comoving-frame radiative transfer equation**.

!!! *Till 1999 CMFGEN didn't have its name*

predecessor of CMFGEN

To facilitate the simultaneous solution of the transfer equations and the statistical equilibrium equations, a partial linearization method is used. Iterative scheme uses a triagonal (or pentadiagonal) Newton-Raphson operator, and is based on complete linearization method of Auer and Michalas (1969). This method is closely related to procedures that use approximate lambda operators and has similar convergence properties.

Hillier (1987, 1990, 1991)

!!! *Till 1999 CMFGEN didn't have its name*

predecessor of CMFGEN

Predecessor of CMFGEN has become widely used for studying Galactic and extragalactic WR stars and even LBVs

Astron. Astrophys. 293, 403–426 (1995)

ASTRONOMY
AND
ASTROPHYSICS

Fundamental parameters of Wolf-Rayet stars

II. Tailored analyses of Galactic WNL stars*

P.A. Crowther¹, D.J. Hillier², and L.J. Smith¹

¹ Department of Physics and Astronomy, University College London, Gower Street, London, WC1E 6BT, UK

² Department of Physics and Astronomy, University of Pittsburgh, 3941 O'Hara Street, Pittsburgh PA 15260, USA

Received 25 April 1994 / Accepted 8 June 1994

Abstract. Quantitative analyses of 9 Galactic WNL (WN7–8) stars, with particular reference to the hydrogen, helium, carbon and nitrogen abundances, are presented. These analyses are based on extensive UV, optical and IR spectroscopy, and have been undertaken using the Wolf-Rayet (WR) standard model.

1. Introduction

The late WN (or WNL) stars are those Wolf-Rayet (WR) stars of the nitrogen sequence which show lines of principally He I–II and N III–IV in their spectra. WNL stars are the most luminous,

!!! Till 1999 CMFGEN didn't have its name

Astron. Astrophys. 302, 830–838 (1995)

ASTRONOMY
AND
ASTROPHYSICS

A detailed study of a very late WN star in M 33*

L.J. Smith, P.A. Crowther, and A.J. Willis

Department of Physics and Astronomy, University College London, Gower Street, London, WC1E 6BT, UK

Received 20 February 1995 / Accepted 23 March 1995

Abstract. We present the first quantitative analysis of a M 33 Wolf-Rayet star, the Ofpe/WN9 candidate MCA1-B (Willis et al. 1992). From new higher resolution observations analysed with the Wolf-Rayet standard model, we reclassify MCA1-B as WN9 and find its stellar parameters ($T_{\text{eff}}=29\text{kK}$, $T_{\text{eff}}=19\text{kK}$, log

the atmosphere to reveal the products of CNO-cycle burning. A direct link between the Ofpe/WN9 stars and the LBVs was established observationally by Stahl et al. (1983) who found that the prototype Ofpe/WN9 star R127 (Walborn 1982) had evolved to a B emission line supergiant (and more recently to a

from predecessor of CMFGEN to CMFGEN

Comparison of observations with model results revealed “weak points” of theoretical assumptions.

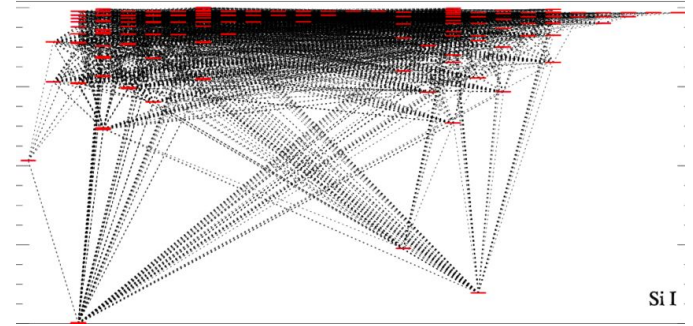
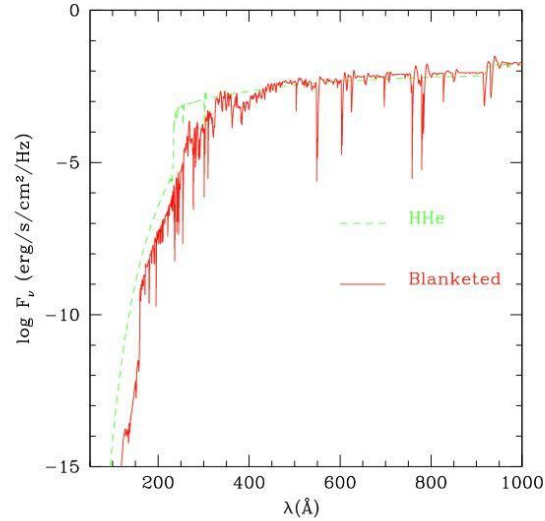
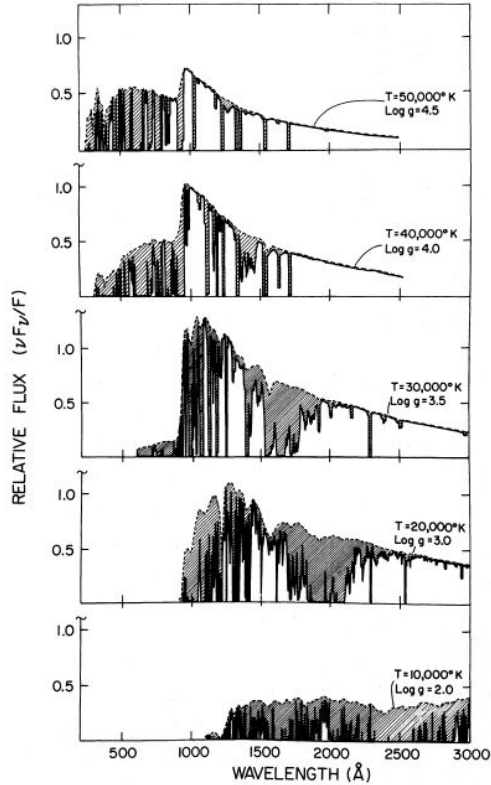
For the next step in modeling – codes should include:

- Line blanketing effect
- Auger ionisation effect
- Clumping

Blanketing

Line blanketing is the enhancement of the red or infrared regions of a stellar spectrum at the expense of the other regions, with an overall diminishing effect on the whole spectrum. The term originates in a 1928 article by astrophysicist Edward Arthur Milne, where it was used to describe the effects that the astronomical metals in a star's outer regions had on that star's spectrum. The name arose because the absorption lines act as a "blanket", causing the continuum temperature of the spectrum to rise over what it would have been if these lines were not present.

Blanketing



Blanketing (as of mid 90s)

- Before 1990-s most codes neglected non-LTE line blanketing.
- All codes in spherical geometry and with radial outflow of material consistently treated only the major species (e.g., H, He, and in some cases CNO) and neglected line blanketing caused by elements of iron group.
- The impact of extreme UV line blocking on the electron populations and ionization structure of the wind quickly became obvious
- In the beginning of 1990-s advances in computing power and computational techniques have led several groups to invest a large effort into including non-LTE line blanketing into plane-parallel static atmospheres.

Blanketing (as of mid 90s)

- Before 1990-s most codes neglected non-LTE line blanketing.
- All codes in spherical geometry and with radial outflow of material consistently treated only the major species (e.g., H, He, and in some cases CNO) and neglected line blanketing caused by elements of iron group.
- The impact of extreme UV line blocking on the electron populations and ionization structure of the wind quickly became obvious
- In the beginning of 1990-s advances in computing power and computational techniques have led several groups to invest a large effort into including non-LTE line blanketing into plane-parallel static atmospheres.
- **Hillier & Millier (1998) were the first to include NLTE-line blanketing in their WR models**

Blanketing

!!! *in 1998 CMFGEN was still a nameless code*

The key aspects of implementation line blanketing in CMFGEN*:

1. Radiative transfer in the lines is treated "exactly", meaning that no opacity redistribution or sampling techniques are used. We still make the usual assumption of complete redistribution in the line.
2. Super levels are used to decrease the number of levels whose atomic populations must be explicitly solved.
3. Level dissolution using a technique similar to that of Hubeny, Hummer, & Lanz (1994) is utilized.

Super-levels

The idea of **super levels** was first pioneered by Anderson (1989). In it, levels with similar excitation energies are grouped together, and within each group, the departure coefficients are assumed to be identical. Only the population (or equivalently, the departure coefficient) of the super level need be solved in order to fully specify the populations of the levels within a super level. This approach is a natural extension of the single-level LTE assumption, and thus LTE is recovered exactly at depth.

- Some ions (e.g., Fe III) have 1000's of atomic levels
- Impracticable to treat all levels in non-LTE. Therefore group levels, & treat as single level in the rate equations. All lines treated at their correct wavelengths.
- Simplest grouping – group terms belonging to same LS state. Reduces # of levels by factor of 3.
- Optimal grouping unknown

Super-levels

Table A.1 Electronic terms for atoms with equivalent-electron configurations

Configuration	Electronic terms	Atoms
$p p^5$	2P	B, F
$p^2 p^4$	$^1S \ ^3P \ ^1D$	C, O, N ⁺
p^3	$^4S \ ^2P \ ^2D$	N, O ⁺
p^6	1S	Ne
$d d^9$	2D	Sc
$d^2 d^8$	$^1S \ ^3P \ ^1D \ ^3F \ ^1G$	Ti, Ni
$d^3 d^7$	$^2P \ ^4P \ ^2D \ ^2F \ ^4F \ ^2G \ ^2H$	V, Co
$d^4 d^6$	$^2^1S \ 2^3P \ 2^1D \ 3^3D \ 5^5D \ 1^1F$ $2^3F \ 2^1G \ 3^3G \ 3^H \ 1^1I$	Fe
d^5	$^2S \ 6^6S \ 2^2P \ 4^4P \ 3^2D \ 4^4D \ 2^2F$ $4^4F \ 2^2G \ 4^4G \ 2^2H \ 2^1I$	Mn
d^{10}	1S	Zn

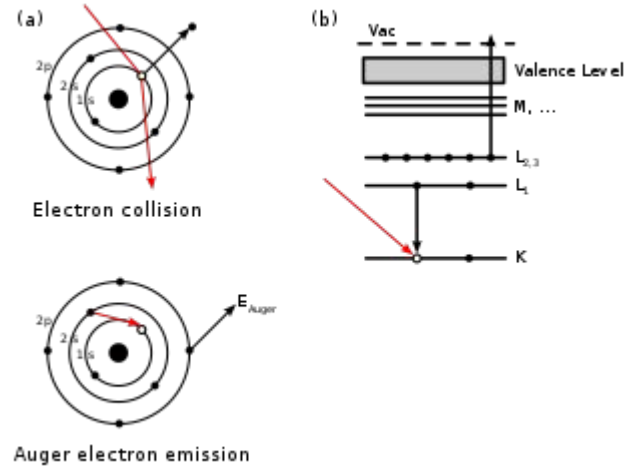
M. Capitelli et al., *Fundamental Aspects of Plasma Chemical Physics: Thermodynamics*,
 231 Springer Series on Atomic, Optical, and Plasma Physics 66,
 DOI 10.1007/978-1-4419-8182-0, © Springer Science+Business Media, LLC 2012

e.g, $3p^3 (^2D) 3d \rightarrow \ ^1,3S \ ^1,3P \ ^1,3D \ ^1,3F \ ^1,3G \quad (18 \text{ levels})$
 $(122 \text{ transitions to } 3p^3 ()4l \text{ states})$

Auger ionization

The **Auger effect** is a physical phenomenon in which the filling of an inner-shell vacancy of an atom is accompanied by the emission of an electron from the same atom. When a core electron is removed, leaving a vacancy, an electron from a higher energy level may fall into the vacancy, resulting in a release of energy.

Early UV observations of hot stars often showed spectral features (e.g., O VI) that were not expected on the basis of the stars effective temperature. It was quickly realized that a possible explanation was Auger ionization (Cassinelli & Olson 1979).



Auger ionization

For an arbitrary ionization stage we have

$$\frac{DN_i}{Dt} = 0 = R_{i,i+1} + X_{i,i+2} - R_{i-1,i} - X_{i-2,i}$$

where

N_i - total population of ionization stage N_i

$R_{i,i+1}$ = net recom. (photoionization and collisional) from ion. $i + 1$ to ion. i

$X_{i,i+2}$ = net X-ray rec. from ionization stage $i + 2$ to ionization stage i .

Thus (for 6 ionization stages) we have

$$0 = R_{1,2} + X_{1,3} \quad (1)$$

$$0 = R_{2,3} + X_{2,4} - R_{1,2} \quad (2)$$

$$0 = R_{3,4} + X_{3,5} - R_{2,3} - X_{1,3} \quad (3)$$

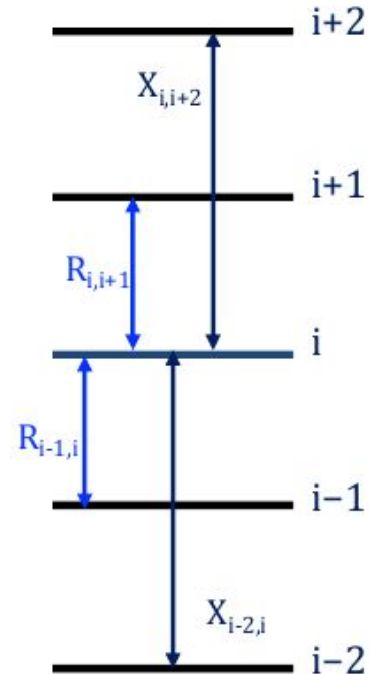
$$0 = R_{4,5} + X_{4,6} - R_{3,4} - X_{2,4} \quad (4)$$

$$0 = R_{5,6} - R_{4,5} - X_{3,5} \quad (5)$$

$$0 = -R_{5,6} - X_{4,6} \quad (6)$$

Can treat equations as written, or simplify for numerical stability.

$$(1) + (2) \implies 0 = R_{2,3} + X_{2,4} + X_{1,3}$$



Clumping

Theoretically, the intrinsic instability of radiation driven winds predicts the formation of shocks and inhomogeneities (clumps)

```
graph TD; A[Theoretically, the intrinsic instability of radiation driven winds predicts the formation of shocks and inhomogeneities (clumps)] --> B[Theory]; A --> C[Observations];
```

Theory

Owocki et al. (1988), Feldmeier et al. (1997), Runacres & Owocki (2002)

Observations

Robert (1994), Hillier (1991)
Eversberg et al. (1998)

Clumping in CMFGEN

CMFGEN include simple filling factor approach. Winds are clumped with a **volume filling factor f** and there is no interclump medium. Clumping affect on mass-loss rates derived from radio fluxes

$$f(r) = a + (1 - a) \exp [-v(r)/b]$$

$$\rho(r) = \frac{\dot{M}}{4\pi r^2 v(r) f(r)}$$

To solve the transfer equation we assume that the clumps are small compared to the mean free path of the photons

Clumping

In this formulation of clumping, the expressions for the opacities and emissivities are

$$[\eta(r), \chi(r)]_{\text{clump}} = [\eta(r), \chi(r)]f(r)$$

where η and χ are computed using populations and densities appropriate to the clumps. The solution of the radiative transfer equation and the equilibrium equations then proceeds exactly as in the unclumped model

Hillier & Miller, 1999

from predecessor of CMFGEN to CMFGEN

THE ASTROPHYSICAL JOURNAL, 496:407–427, 1998 March 20
© 1998. The American Astronomical Society. All rights reserved. Printed in U.S.A.

Hillier & Miller, 1998, ApJ, 496, 407-427

THE TREATMENT OF NON-LTE LINE BLANKETING IN SPHERICALLY EXPANDING OUTFLOWS

D. JOHN HILLIER

Department of Physics and Astronomy, University of Pittsburgh, Pittsburgh, PA 15260

AND

D. L. MILLER

Steward Observatory, University of Arizona, Tucson,
Received 1997 March 6; accepted 1997 October

ABSTRACT

Extensive modifications to the non-LTE radiative transfer code of
improve the spectroscopic analysis of stars with stellar winds. The m
inclusion of blanketing due to thousands of overlapping lines. To imp
idea of super levels first pioneered by Anderson. In our approach, le
and levels are grouped together. Within this group, we assume that t
col. Only the population (or equivalently, the departure coefficient)

THE ASTROPHYSICAL JOURNAL, 519:354–371, 1999 July 1
© 1999. The American Astronomical Society. All rights reserved. Printed in U.S.A.

CONSTRAINTS ON THE EVOLUTION OF MASSIVE STARS THROUGH SPECTRAL ANALYSIS. I. THE WC5 STAR HD 165763

D. JOHN HILLIER

Department of Physics and Astronomy, University of Pittsburgh, Pittsburgh, PA 15260

AND

D. L. MILLER

Steward Observatory, University of Arizona, Tucson, AZ 85721
Received 1998 May 29; accepted 1999 February 3

ABSTRACT

Using a significantly revised non-LTE radiative transfer code that allows for the effects of line blanket-
g by He, C, O, Si, and Fe, we have performed a detailed analysis of the Galactic Wolf-Rayet (W-R)
ir HD 165763 (WR 111, WC5). Standard W-R models consistently overestimate the strength of the
ctron scattering wings, especially on strong lines, so we have considered models where the wind is
th homogeneous and clumped. The deduced stellar parameters for HD 165763 are as follows:

$$L = 2.0 \times 10^5 L_{\odot}, \quad R_{*} = 1.8 R_{\odot}, \quad \dot{M} = 1.5 \times 10^{-5} M_{\odot} \text{ yr}^{-1}, \quad V_{\infty} = 2300 \text{ km s}^{-1},$$

0.154 .

tor of the clumps is assumed
nilar results are obtained for

Line Blanketing
Auger Effect

Clumping

!!! in 1999 CMFGEN was still a nameless code

Hillier & Miller, 1999, ApJ, 519, 354-371

from predecessor of CMFGEN to CMFGEN

Crowther et al. 1999 “Wolf-Rayet nebulae as tracers of stellar ionizing fluxes. I. M1-67”

ASTRONOMY
AND
ASTROPHYSICS

Wolf-Rayet nebulae as tracers of stellar ionizing fluxes

I. M1-67

Paul A. Crowther¹, A. Pasquali², Orsola De Marco^{1,3}, W. Schmutz³,

¹ Department of Physics and Astronomy, University College London, Gower St

² ST-ECF/ESO, Karl-Schwarzschild-Strasse 2, 85748 Garching bei München, G

³ Institut für Astronomie, ETH-Zentrum, 8092 Zürich, Switzerland

⁴ Physikalisch-Meteorologisches Observatorium Davos, 7260 Davos Dorf, Swit

⁵ Department of Physics and Astronomy, University of Pittsburgh, 3941 O'Hara

⁶ Astronomical Institute 'Anton Pannekoek', University of Amsterdam, Kruislaan

Received 2 June 1999 / Accepted 25 August 1999

Abstract. We use WR124 (WN8h) and its associated nebula M1-67, to test theoretical non-LTE models for Wolf-Rayet (WR) stars. Lyman continuum ionizing flux distributions derived from a stellar analysis of WR124, are compared with nebular properties via photo-ionization modelling. Our study demonstrates the significant role that line blanketing plays in

3. Stellar atmosphere codes

In this section we introduce and utilise the codes that are used to carry out spectral synthesis of WR124. **CMFGEN** (Hillier 1987, 1990; Hillier & Miller 1998, 1999) solves the transfer equation in the co-moving frame, subject to statistical and radiative equilibrium, assuming an expanding, spherically-symmetric, homogeneous or clumped, atmosphere. Populations and ionization structure are consistent with the radiation field.

1. Intro

The Lyman ionizing energy distributions of hot, massive stars are important in the study of young starburst regions and galaxies, via population synthesis codes (e.g. Leitherer et al. 1999). However, the interstellar medium (ISM) conspires to prevent this energy from reaching the Earth's atmosphere. Interstellar

CMFGEN

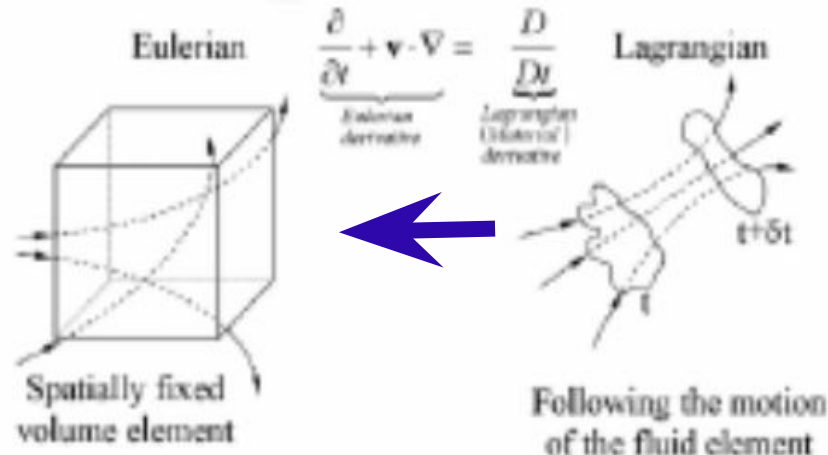
The code assumes spherical symmetry, stationary outflow, and what both photospheric and wind lines may be treated in non-LTE. Full line blanketing due to hundreds of thousands of spectral lines is included, as well as wind clumping.

CMFGEN comprises not only a single executable, and actually a suite of codes are used in the process of analyzing stellar spectra. While the temperature, atmospheric and wind structures, and level populations are obtained with **CMFGEN** itself, the observed spectrum is computed with a separate code (**CMF_FLUX**). Many accompanying routines for plotting and analysis (**DISPGEN** and **PLT_SPEC**) and computation of Rosseland opacities (**MAIN_LTE**), among others, are provided.

CMF_FLUX

CMF_FLUX is an one-dimensional code to compute synthetic spectra in the observer's frame, what is used with CMFGEN to compute synthetic spectra

CMF_FLUX calculates synthetic spectra in the observer's frame simultaneously with the solution of the statistical and radiative equilibrium equations using CMFGEN. Basically, the outer boundary intensity in the comoving frame is transformed to the observer's frame for each impact parameter



CMF_FLUX: Difficulties

Three difficulties present themselves with the observer's-frame calculation:

- effects of electron scattering need
- lot of bookkeeping involved because of overlapping lines and the Doppler shifts.
- along a ray a single line interacts only over a few Sobolev lengths, a distance that can be much smaller than the grid spacing

CMF_FLUX

Several additional options are provided in CMF_FLUX:

1. One can calculate a pure continuum spectrum, although it should be noted that the definition of continuum is problematic. Strong resonances in the photoionization cross sections can appear either as narrow or broad features in the continuum spectrum.
2. Line spectra for individual species or ions can be computed.
3. It is possible to output $I(\nu, \rho)$ at the outer boundary. This information, equivalent to the limb-darkening law, is useful for interpreting interferometric measurements.
4. The depth variation of the flux, opacities, emissivities, and force multiplier can be output to direct-access files. An auxiliary plot program is available to help interpret these files.
5. It is possible to compute the EWs of strong emission lines using the Sobolev approximation (useful for Wolf-Rayet stars and luminous blue variables)
6. It is possible to alter the abundance of an impurity species in order to obtain a zeroth-order estimate of the effects of abundance changes.

CMF_FLUX

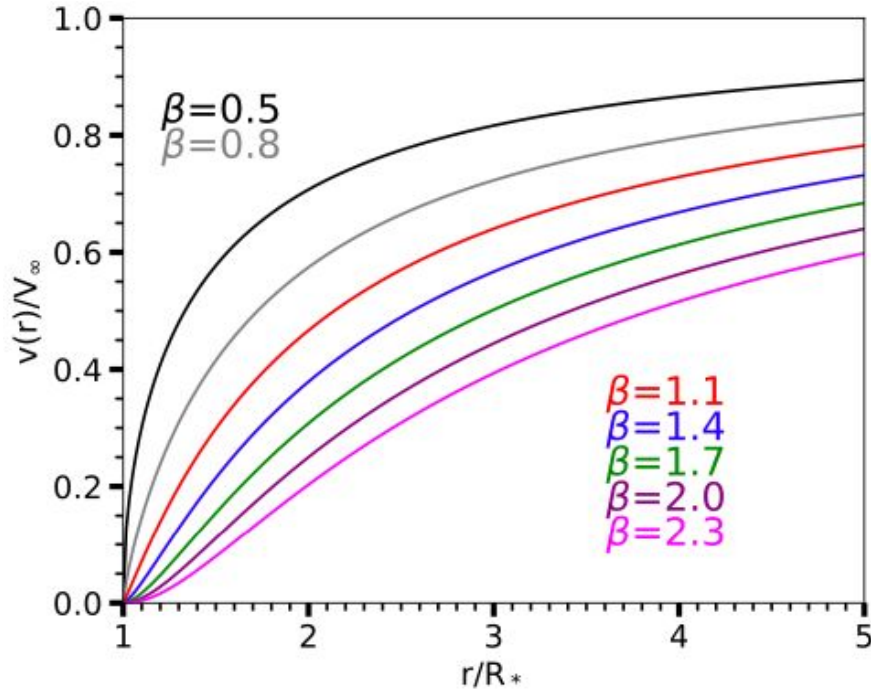
Several additional options are provided in CMF_FLUX:

1. One can calculate a pure continuum spectrum, although it should be noted that the definition of continuum is problematic. Strong resonances in the photoionization cross sections can appear either as narrow or broad features in the continuum spectrum.
2. Line spectra for individual species or ions can be computed.
3. It is possible to output $I(\nu, \rho)$ at the outer boundary. This information, equivalent to the limb-darkening law, is useful for interpreting interferometric measurements.
4. The depth variation of the flux, opacities, emissivities, and force multiplier can be output to direct-access files. An auxiliary plot program is available to help interpret these files.
5. It is possible to compute the EWs of strong emission lines using the Sobolev approximation (useful for Wolf-Rayet stars and luminous blue variables)
6. It is possible to alter the abundance of an impurity species in order to obtain a zeroth-order estimate of the effects of abundance changes.

Busche & Hillier, 2005

Velocity Law

CMFGEN does not solve the hydrodynamic equations of the wind \rightarrow a velocity law has to be assumed *a priori*. Simple parametric *beta law* approximation is used



$$v(r) = v_\infty \left(1 - R/r\right)^\beta,$$

$\beta = 0.5$ (CAK case)

$\beta = 0.8$ (O-stars) ... 2 (BA-supergiants)

Atomic Data

Atomic data

quality and self-consistency of atomic data plays a key role in the spectroscopic analysis and determination of stellar parameters.

The atomic data contained in CMFGEN comes from a variety of sources, which are mainly the Opacity Project, the NIST database, and from several individuals such as Robert Kurucz, Keith Butler, Sultana Nahar & Anil Prandham, and Gary Ferland.

CMFGEN stores atomic data in ASCII files in unique directory structures, with separate files containing collisional cross sections, oscillator strengths and energy levels, auto ionization rates, superlevels designation, and photoionization cross sections from the ground and excited states. The atomic data format is unique to CMFGEN, and conversion from published data into CMFGEN is time consuming. Unfortunately, this hampers the portability of atomic data and test models using atomic datasets from different groups has been done on a very limited basis

CMFGEN application: Wolf–Rayet Stars

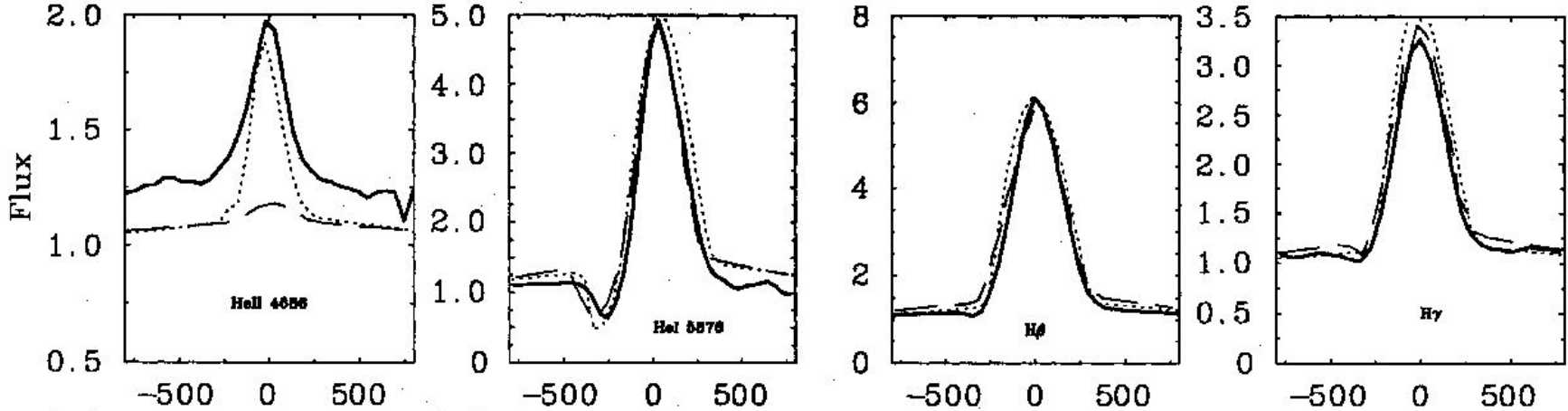
Paul Crowther

Crowther et al. +

- 1995 "Fundamental parameters of Wolf–Rayet stars. I Ofpe/WN9 stars"
- 1994 "Fundamental parameters of Wolf–Rayet stars. II Tailored analyses of Galactic WNL stars"
- 1995 "Fundamental parameters of Wolf–Rayet stars. III Evolution status of WNL stars"
- Crowther et al. 1995 "Fundamental parameters of Wolf–Rayet stars. IV. Weak-lined WNE stars"
- 1995 "Fundamental parameters of Wolf–Rayet stars. V. The nature of the WN/C star WR 8"
- 1997 Fundamental parameters of Wolf–Rayet stars. VI. Large Magellanic Cloud WNL stars

CMFGEN application: Wolf-Rayet Stars

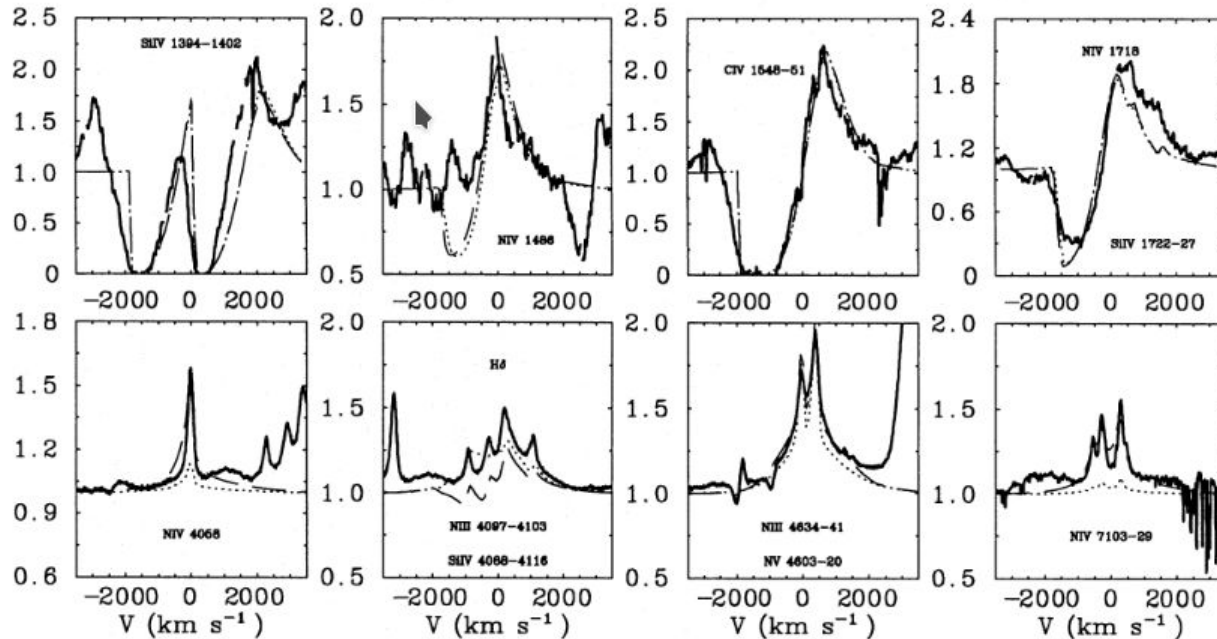
Fit for Sk66°-40 (WN10)



Crowther et al. 1995 "Fundamental parameters of Wolf-Rayet stars. I Ofpe/WN9 stars"

CMFGEN application: Wolf-Rayet Stars

Fit for WR22 (WN7+abs)

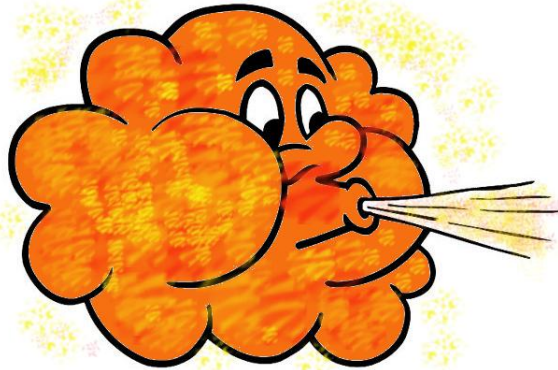


Crowther et al. 1994 "Fundamental parameters of Wolf-Rayet stars. II Tailored analyses of Galactic WNL stars"

CMFGEN application: Wolf-Rayet Stars

Crowther et al. 1995 "Fundamental parameters of Wolf-Rayet stars. III Evolution status of WNL stars"

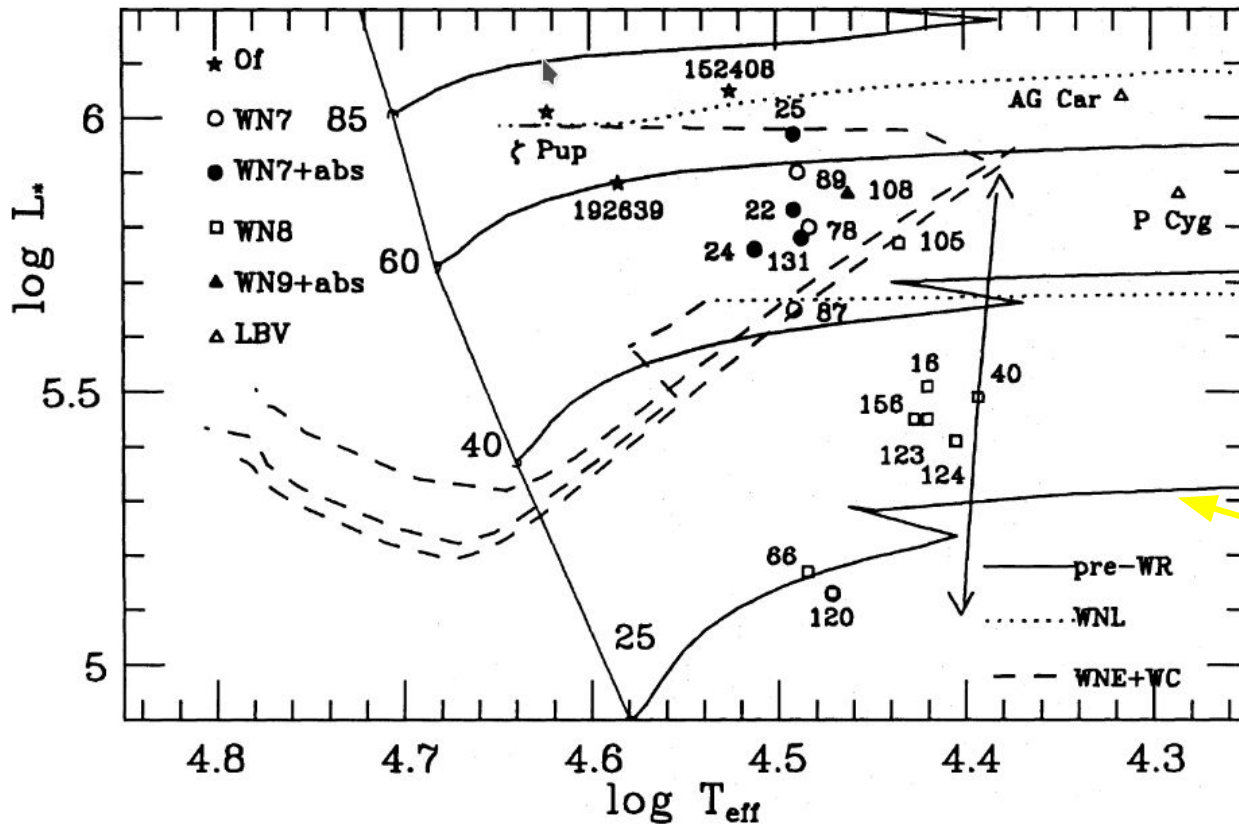
T_* , T_{eff} , L_* , \dot{M} , V_∞ ,
 X_H , X_{He} , X_C , X_N



WR	Star	Subtype	T_* (kK)	T_{eff} (kK)	$R_{2/3}$ (R_\odot)	$\log L_*$ (L_\odot)	M (M_\odot)	$\log \dot{M}$	v_∞	$\frac{\dot{M} v_\infty}{L_* / c}$	H/He (#)	N/He (#)	C/N (#)	M_v	Ref
	ζ Pup	O4I(n)f	...	42.1	19.0	6.0	30:	-5.4	2200	0.4	5.0	0.005	0.12	-6.0	1,2,9,10
	HD 192639	O7Ib(f)	...	38.5	19.5	5.9	31:	-5.5	2180	0.4	4.0	-6.2	3,5
	HD 152408	O8:1afpe	...	33.5	31.0	6.0	60?	-4.7	960	0.8	-7.0	4,6,11
22	HD 92740	WN7+abs	31.9	31.2	28.5	5.8	37:	-4.3	1785	7	3.2	0.005	0.04	-6.8	14
24	HD 93131	WN7+abs	33.3	32.5	23.9	5.8	35:	-4.3	2160	9	3.2	0.004	0.08	-6.5	14
25	HD 93162	WN7+abs	31.2	31.0	33.3	6.0	54:	-4.4	2480	5	4.5	0.003	0.08	-7.2	14
131	MR 97	WN7+abs	31.4	30.7	27.5	5.8	25?	-4.3	1400	5.7	1.0	-6.7	7
78	HD 151932	WN7	33.6	30.4	28.6	5.8	20?	-4.1	1385	9	0.5	0.005	0.02	-6.6	14
87	LSS 4064	WN7(+abs?)	31.3	31.0	23.4	5.7	20?	-4.6	1400	3.8	2.7	-6.4	7
89	LSS 4065	WN7(+abs?)	31.2	30.8	31.4	5.9	30?	-4.2	1600	5.6	1.0	-7.0	7
120	MR 89	WN7-8	34.5	29.6	14.0	5.1	8:	-4.3	1225	20	<0.2	-5.1	14
16	HD 86161	WN8	34.5	26.3	26.7	5.5	13	-4.2	630	6	1.0	0.006	0.01	-6.0	14
40	HD 96548	WN8	35.9	24.7	30.4	5.5	13	-4.0	840	13	0.75	0.006	0.01	-6.0	14
123	HD 177230	WN8	33.9	26.3	25.5	5.4	13	-4.0	970	16	<0.1	0.005	0.02	-6.0	14
124	209 BAC	WN8	33.5	25.4	26.2	5.4	12	-4.1	710	10	0.6	0.004	0.01	-5.9	14
156	MR 119	WN8	31.8	26.7	24.8	5.4	13	-4.4	660	5	1.5	0.007	0.14	-6.0	14
108	HDE 313846	WN9+abs	29.9	29.0	33.6	5.9	50:	-4.3	1170	4	1.5	0.010	0.10:	-7.1	13
LBV	AG Car	WN11	26.0	20.7	81.7	6.0	32:	-4.3	250	0.6	2.4	-7.7	8
LBV	P Cyg	B1Ia ⁺	...	19.3	76.0	5.9	23:	-4.5	185	0.4	2.5	12
40 M_\odot	(stage 33)		42.3	19.9	58.0	5.7	19	-4.4	—	—	2.5	0.006	0.02		
60 M_\odot	(stage 22)		28.1	19.2	99.8	6.1	35	-4.4	—	—	1.0	0.005	0.03		
85 M_\odot	(stage 19)		23.8	17.9	142.0	6.3	52	-4.4	—	—	1.5	0.006	0.03		

(1) Groenewegen & Lamers (1989); (2) Bohannon et al. (1990); (3) Prinja et al. (1990); (4) Leitherer & Robert (1991); (5) Herrero et al. (1992); (6) Lamers & Leitherer (1993); (7) Hamann et al. (1994); (8) Smith et al. (1994); (9) Pauldrach et al. (1994); (10) Schaerer & Schmutz (1994); (11) Prinja & Fullerton (1994); (12) Langer et al. (1994); (13) Paper I; (14) Paper II.

CMFGEN application: Wolf-Rayet Stars



Crowther et al. 1995
“Fundamental parameters
of Wolf-Rayet stars. III
Evolution status of WNL
stars”

Evolutionary tracks from
Schaller et al. (1992)

CMFGEN application: O-type stars

Since beginning of 2000-s CMFGEN is actively used for modeling O-type stars

Fabrice Martins, Jean-Claude Bouret, Wagner Marcolino

A&A 498, 837–852 (2009)
DOI: [10.1051/0004-6361/200811289](https://doi.org/10.1051/0004-6361/200811289)
© ESO 2009

**Astronomy
&
Astrophysics**

**Analysis of Galactic late-type O dwarfs:
more constraints on the weak wind problem^{*,**}**

W. L. F. Marcolino¹, J.-C. Bouret¹, F. Martins², D. J. Hillier³, T. Lanz⁴, and C. Escolano¹

**Astronomy
&
Astrophysics**

A&A 441, 735–762 (2005)
DOI: [10.1051/0004-6361:20052927](https://doi.org/10.1051/0004-6361:20052927)
© ESO 2005

**Lower mass loss rates in O-type stars: Spectral signatures
of dense clumps in the wind of two Galactic O4 stars^{*}**

J.-C. Bouret¹, T. Lanz², and D. J. Hillier³

O stars with weak winds: the Galactic case^{*}

F. Martins^{1,2,3}, D. Schaerer^{1,2}, D. J. Hillier⁴, F. Meynadier⁵, M. Heydari-Malayeri⁵, and N. R. Walborn⁶

CMFGEN application: O-type stars

Martins, Schaerer, Hillier, 2005, “A new calibration of stellar parameters of Galactic O stars”

Supergiants, luminosity class I stars

ST	T_{eff} [K]	$\log g_{\text{spec}}$ [cm s ⁻²]	M_V	BC	$\log \frac{L}{L_{\odot}}$	R [R_{\odot}]	M_{spec} [M_{\odot}]
3	42 551	3.73	-6.35	-3.89	6.00	18.47	66.89
4	40 702	3.65	-6.34	-3.76	5.94	18.91	58.03
5	38 520	3.57	-6.33	-3.60	5.87	19.48	50.87
5.5	37 070	3.52	-6.33	-3.48	5.82	19.92	48.29
6	35 747	3.48	-6.32	-3.38	5.78	20.33	45.78
6.5	34 654	3.44	-6.31	-3.29	5.74	20.68	43.10
7	33 326	3.40	-6.31	-3.17	5.69	21.14	40.91
7.5	31 913	3.36	-6.30	-3.04	5.64	21.69	39.17
8	31 009	3.32	-6.30	-2.96	5.60	22.03	36.77
8.5	30 504	3.28	-6.29	-2.91	5.58	22.20	33.90
9	29 569	3.23	-6.29	-2.82	5.54	22.60	31.95
9.5	28 430	3.19	-6.28	-2.70	5.49	23.11	30.41

Theoretical

Dwarfs, luminosity class V stars

ST	T_{eff} [K]	$\log g_{\text{spec}}$ [cm s ⁻²]	M_V	BC	$\log \frac{L}{L_{\odot}}$	R [R_{\odot}]	M_{spec} [M_{\odot}]
3	44 616	3.92	-5.79	-4.03	5.83	13.84	58.34
4	43 419	3.92	-5.50	-3.95	5.68	12.31	46.16
5	41 540	3.92	-5.21	-3.82	5.51	11.08	37.28
5.5	40 062	3.92	-5.07	-3.71	5.41	10.61	34.17
6	38 151	3.92	-4.92	-3.57	5.30	10.23	31.73
6.5	36 826	3.92	-4.77	-3.47	5.20	9.79	29.02
7	35 531	3.92	-4.63	-3.36	5.10	9.37	26.52
7.5	34 419	3.92	-4.48	-3.27	5.00	8.94	24.15
8	33 383	3.92	-4.34	-3.18	4.90	8.52	21.95
8.5	32 522	3.92	-4.19	-3.10	4.82	8.11	19.82
9	31 524	3.92	-4.05	-3.01	4.72	7.73	18.03
9.5	30 488	3.92	-3.90	-2.91	4.62	7.39	16.46

Theoretical

CMFGEN application: O-type stars

Martins, Schaerer, Hillier, 2005, “A new calibration of stellar parameters of Galactic O stars”

Supergiants, luminosity class I stars

ST	T_{eff} [K]	$\log g_{\text{spec}}$ [cm s ⁻²]	M_V	BC	$\log \frac{L}{L_{\odot}}$	R [R_{\odot}]	M_{spec} [M_{\odot}]
3	42 233	3.73	-6.35	-3.87	5.99	18.56	67.53
4	40 422	3.65	-6.34	-3.74	5.93	18.99	58.54
5	38 612	3.57	-6.33	-3.61	5.87	19.45	50.72
5.5	37 706	3.52	-6.33	-3.54	5.84	19.70	47.25
6	36 801	3.48	-6.32	-3.46	5.81	19.95	44.10
6.5	35 895	3.44	-6.31	-3.39	5.78	20.22	41.20
7	34 990	3.40	-6.31	-3.31	5.75	20.49	38.44
7.5	34 084	3.36	-6.30	-3.24	5.72	20.79	36.00
8	33 179	3.32	-6.30	-3.16	5.68	21.10	33.72
8.5	32 274	3.28	-6.29	-3.08	5.65	21.41	31.54
9	31 368	3.23	-6.29	-2.99	5.61	21.76	29.63
9.5	30 463	3.19	-6.28	-2.91	5.57	22.11	27.83

Observational

Dwarfs, luminosity class V stars

ST	T_{eff} [K]	$\log g_{\text{spec}}$ [cm s ⁻²]	M_V	BC	$\log \frac{L}{L_{\odot}}$	R [R_{\odot}]	M_{spec} [M_{\odot}]
3	44 852	3.92	-5.79	-4.05	5.84	13.80	57.95
4	42 857	3.92	-5.50	-3.91	5.67	12.42	46.94
5	40 862	3.92	-5.21	-3.77	5.49	11.20	38.08
5.5	39 865	3.92	-5.07	-3.70	5.41	10.64	34.39
6	38 867	3.92	-4.92	-3.62	5.32	10.11	30.98
6.5	37 870	3.92	-4.77	-3.55	5.23	9.61	28.00
7	36 872	3.92	-4.63	-3.47	5.14	9.15	25.29
7.5	35 874	3.92	-4.48	-3.39	5.05	8.70	22.90
8	34 877	3.92	-4.34	-3.30	4.96	8.29	20.76
8.5	33 879	3.92	-4.19	-3.22	4.86	7.90	18.80
9	32 882	3.92	-4.05	-3.13	4.77	7.53	17.08
9.5	31 884	3.92	-3.90	-3.04	4.68	7.18	15.55

Observational

CMFGEN application: O-type stars

Martins, Plez, 2006, “UBVJHK synthetic photometry of Galactic O stars”

ST	M_U	M_B	M_V	M_J	M_H	M_K	$(U - B)_0$	$(B - V)_0$	$(J - H)_0$	$(H - K)_0$	BC_U	BC_B	BC_V	BC_J	BC_H	BC_K
O3V	-7.31	-6.15	-5.86	-5.19	-5.07	-4.98	-1.16	-0.28	-0.11	-0.10	-2.54	-3.70	-3.99	-4.66	-4.78	-4.87
O4V	-7.01	-5.85	-5.57	-4.91	-4.79	-4.69	-1.15	-0.28	-0.11	-0.10	-2.42	-3.57	-3.85	-4.52	-4.63	-4.73
O5V	-6.69	-5.54	-5.27	-4.60	-4.49	-4.39	-1.14	-0.28	-0.11	-0.10	-2.29	-3.43	-3.71	-4.37	-4.48	-4.58
O5.5V	-6.56	-5.42	-5.14	-4.48	-4.37	-4.27	-1.14	-0.28	-0.11	-0.10	-2.22	-3.36	-3.64	-4.29	-4.40	-4.50
O6V	-6.40	-5.27	-4.99	-4.34	-4.22	-4.13	-1.13	-0.28	-0.11	-0.10	-2.15	-3.28	-3.56	-4.21	-4.33	-4.42
O6.5V	-6.24	-5.12	-4.84	-4.19	-4.08	-3.98	-1.13	-0.27	-0.11	-0.10	-2.08	-3.21	-3.48	-4.13	-4.24	-4.34
O7V	-6.09	-4.97	-4.70	-4.05	-3.94	-3.84	-1.12	-0.27	-0.11	-0.10	-2.01	-3.13	-3.40	-4.05	-4.16	-4.26
O7.5V	-5.94	-4.83	-4.56	-3.91	-3.80	-3.70	-1.11	-0.27	-0.11	-0.10	-1.93	-3.05	-3.32	-3.96	-4.07	-4.17
O8V	-5.79	-4.68	-4.41	-3.78	-3.67	-3.57	-1.11	-0.27	-0.11	-0.10	-1.86	-2.97	-3.24	-3.87	-3.98	-4.08
O8.5V	-5.62	-4.52	-4.25	-3.62	-3.51	-3.41	-1.10	-0.27	-0.11	-0.10	-1.78	-2.88	-3.15	-3.78	-3.89	-3.99
O9V	-5.48	-4.38	-4.12	-3.48	-3.38	-3.28	-1.10	-0.27	-0.11	-0.10	-1.70	-2.79	-3.06	-3.69	-3.80	-3.90
O9.5V	-5.34	-4.25	-3.98	-3.36	-3.25	-3.15	-1.09	-0.26	-0.11	-0.10	-1.61	-2.70	-2.97	-3.59	-3.70	-3.80
O3III	-7.63	-6.47	-6.18	-5.51	-5.40	-5.30	-1.16	-0.28	-0.11	-0.10	-2.52	-3.68	-3.97	-4.64	-4.75	-4.85
O4III	-7.49	-6.33	-6.05	-5.39	-5.27	-5.18	-1.15	-0.28	-0.11	-0.10	-2.39	-3.54	-3.82	-4.49	-4.60	-4.70
O5III	-7.33	-6.18	-5.91	-5.25	-5.14	-5.04	-1.14	-0.28	-0.11	-0.10	-2.25	-3.39	-3.67	-4.33	-4.44	-4.54
O5.5III	-7.25	-6.11	-5.84	-5.18	-5.07	-4.97	-1.14	-0.28	-0.11	-0.10	-2.18	-3.31	-3.59	-4.24	-4.36	-4.46
O6III	-7.17	-6.04	-5.77	-5.12	-5.00	-4.91	-1.13	-0.27	-0.11	-0.10	-2.10	-3.23	-3.51	-4.16	-4.27	-4.37
O6.5III	-7.07	-5.95	-5.68	-5.03	-4.92	-4.82	-1.12	-0.27	-0.11	-0.10	-2.03	-3.15	-3.42	-4.07	-4.18	-4.28
O7III	-7.00	-5.88	-5.61	-4.97	-4.86	-4.76	-1.12	-0.27	-0.11	-0.10	-1.95	-3.07	-3.34	-3.98	-4.09	-4.19
O7.5III	-6.93	-5.82	-5.55	-4.91	-4.80	-4.70	-1.11	-0.27	-0.11	-0.10	-1.87	-2.98	-3.25	-3.89	-4.00	-4.10
O8III	-6.84	-5.74	-5.47	-4.83	-4.72	-4.62	-1.10	-0.27	-0.11	-0.10	-1.79	-2.89	-3.16	-3.79	-3.90	-4.00
O8.5III	-6.75	-5.65	-5.39	-4.76	-4.65	-4.55	-1.10	-0.27	-0.11	-0.10	-1.70	-2.80	-3.06	-3.69	-3.80	-3.90
O9III	-6.66	-5.58	-5.31	-4.68	-4.58	-4.48	-1.09	-0.26	-0.11	-0.10	-1.61	-2.70	-2.96	-3.59	-3.70	-3.80
O9.5III	-6.60	-5.52	-5.26	-4.64	-4.53	-4.43	-1.08	-0.26	-0.11	-0.10	-1.52	-2.60	-2.86	-3.48	-3.59	-3.69

Observational

CMFGEN application: O-type stars

Martins, Plez, 2006, “UBVJHK synthetic photometry of Galactic O stars”

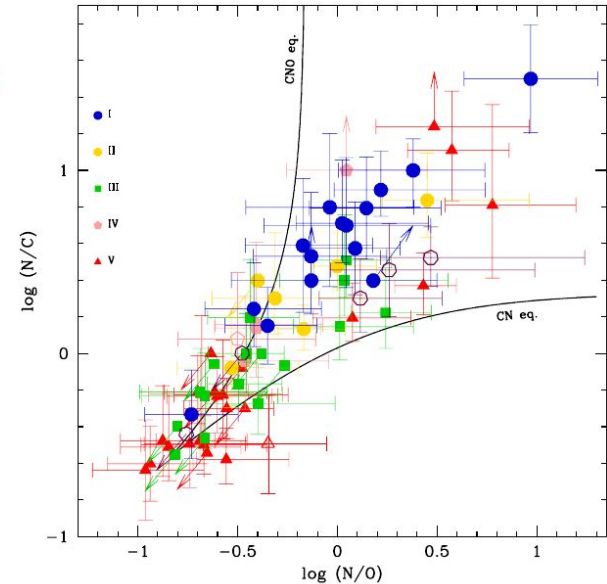
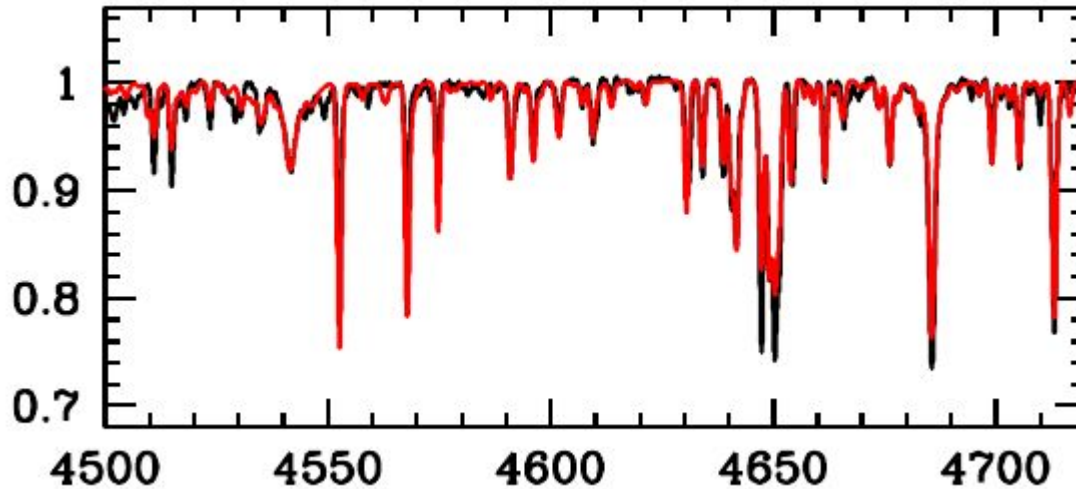
ST	M_U	M_B	M_V	M_J	M_H	M_K	$(U - B)_0$	$(B - V)_0$	$(J - H)_0$	$(H - K)_0$	BC_U	BC_B	BC_V	BC_J	BC_H	BC_K
O3V	-7.30	-6.14	-5.85	-5.18	-5.07	-4.97	-1.16	-0.28	-0.11	-0.10	-2.52	-3.69	-3.97	-4.65	-4.76	-4.86
O4V	-7.00	-5.84	-5.56	-4.89	-4.78	-4.68	-1.16	-0.28	-0.11	-0.10	-2.45	-3.61	-3.89	-4.56	-4.67	-4.77
O5V	-6.69	-5.55	-5.27	-4.60	-4.49	-4.39	-1.15	-0.28	-0.11	-0.10	-2.33	-3.48	-3.76	-4.42	-4.53	-4.63
O5.5V	-6.54	-5.40	-5.12	-4.47	-4.35	-4.26	-1.14	-0.28	-0.11	-0.10	-2.23	-3.37	-3.65	-4.31	-4.42	-4.52
O6V	-6.40	-5.27	-5.00	-4.34	-4.23	-4.13	-1.13	-0.27	-0.11	-0.10	-2.10	-3.23	-3.50	-4.16	-4.27	-4.37
O6.5V	-6.25	-5.12	-4.85	-4.20	-4.09	-3.99	-1.12	-0.27	-0.11	-0.10	-2.00	-3.13	-3.40	-4.05	-4.16	-4.26
O7V	-6.09	-4.98	-4.71	-4.07	-3.96	-3.86	-1.11	-0.27	-0.11	-0.10	-1.91	-3.02	-3.29	-3.93	-4.04	-4.14
O7.5V	-5.93	-4.82	-4.55	-3.92	-3.81	-3.71	-1.11	-0.27	-0.11	-0.10	-1.82	-2.93	-3.20	-3.83	-3.94	-4.04
O8V	-5.76	-4.66	-4.40	-3.76	-3.65	-3.55	-1.10	-0.27	-0.11	-0.10	-1.74	-2.84	-3.10	-3.74	-3.85	-3.95
O8.5V	-5.63	-4.54	-4.27	-3.64	-3.53	-3.44	-1.09	-0.26	-0.11	-0.10	-1.67	-2.76	-3.03	-3.66	-3.77	-3.86
O9V	-5.47	-4.38	-4.12	-3.49	-3.38	-3.28	-1.09	-0.26	-0.11	-0.10	-1.58	-2.67	-2.93	-3.56	-3.67	-3.77
O9.5V	-5.31	-4.23	-3.97	-3.35	-3.24	-3.14	-1.08	-0.26	-0.11	-0.10	-1.49	-2.57	-2.83	-3.45	-3.56	-3.66
O3III	-7.63	-6.47	-6.19	-5.52	-5.41	-5.31	-1.16	-0.28	-0.11	-0.10	-2.42	-3.58	-3.86	-4.53	-4.64	-4.74
O4III	-7.47	-6.33	-6.05	-5.38	-5.27	-5.17	-1.15	-0.28	-0.11	-0.10	-2.33	-3.47	-3.75	-4.42	-4.53	-4.63
O5III	-7.30	-6.17	-5.89	-5.24	-5.12	-5.02	-1.14	-0.28	-0.11	-0.10	-2.20	-3.33	-3.61	-4.26	-4.38	-4.48
O5.5III	-7.23	-6.11	-5.83	-5.18	-5.07	-4.97	-1.13	-0.27	-0.11	-0.10	-2.09	-3.22	-3.49	-4.14	-4.25	-4.35
O6III	-7.16	-6.04	-5.76	-5.12	-5.01	-4.91	-1.12	-0.27	-0.11	-0.10	-1.99	-3.11	-3.39	-4.03	-4.14	-4.24
O6.5III	-7.06	-5.95	-5.67	-5.03	-4.92	-4.82	-1.11	-0.27	-0.11	-0.10	-1.92	-3.03	-3.30	-3.94	-4.05	-4.15
O7III	-6.99	-5.88	-5.61	-4.97	-4.86	-4.76	-1.11	-0.27	-0.11	-0.10	-1.84	-2.95	-3.21	-3.85	-3.96	-4.06
O7.5III	-6.90	-5.80	-5.54	-4.90	-4.79	-4.69	-1.10	-0.27	-0.11	-0.10	-1.75	-2.85	-3.11	-3.75	-3.86	-3.96
O8III	-6.83	-5.73	-5.47	-4.84	-4.73	-4.63	-1.09	-0.26	-0.11	-0.10	-1.67	-2.77	-3.03	-3.66	-3.77	-3.87
O8.5III	-6.75	-5.66	-5.40	-4.77	-4.67	-4.57	-1.09	-0.26	-0.11	-0.10	-1.60	-2.69	-2.95	-3.58	-3.68	-3.78
O9III	-6.66	-5.58	-5.32	-4.70	-4.59	-4.49	-1.08	-0.26	-0.11	-0.10	-1.52	-2.60	-2.86	-3.48	-3.59	-3.69
O9.5III	-6.58	-5.50	-5.24	-4.62	-4.51	-4.42	-1.08	-0.26	-0.11	-0.10	-1.47	-2.55	-2.81	-3.43	-3.54	-3.63

Theoretical

CMFGEN application: O-type stars: CNO abundances

CMFGEN is widely used for estimation of CNO abundances, for example

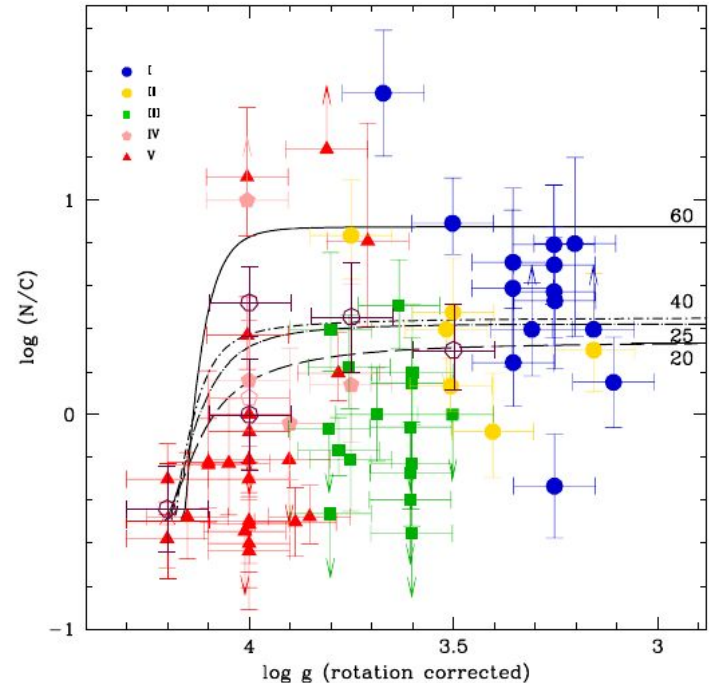
Martins et al., 2015 “*The MiMeS Survey of Magnetism in Massive Stars: CNO surface abundances of Galactic O stars*” → 74 stars from O4 to O9.7



CMFGEN application: O-type stars: CNO abundances

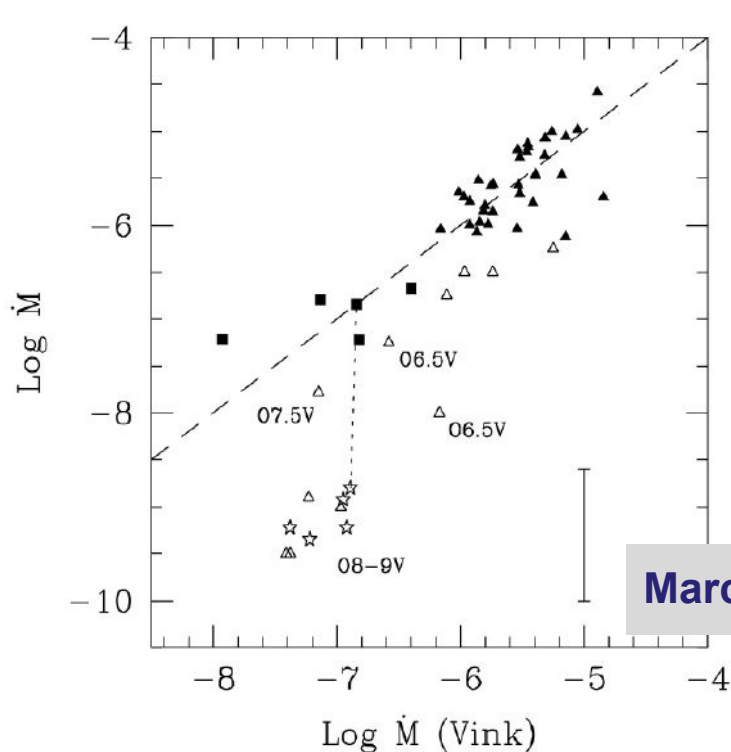
Martins et al., 2015 “*The MiMeS Survey of Magnetism in Massive Stars: CNO surface abundances of Galactic O stars*”

CNO abundances are observed in the range of values predicted by nucleosynthesis through the CNO cycle. More massive stars, within a given luminosity class, appear to be more chemically enriched than lower mass stars. 80% of the sample can be explained by stellar evolution including rotation.

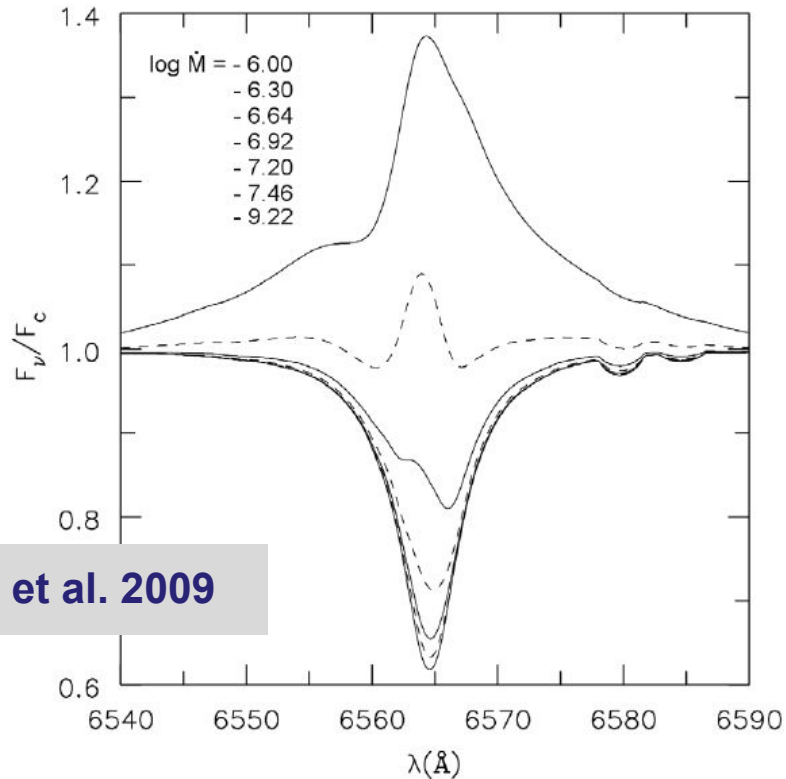


CMFGEN application: O-type stars: Weak wind problem

O dwarfs have been found to have very low mass-loss rates; rates much lower than predicted by theory (the weak wind problem)



Marcolino et al. 2009



CMFGEN application: O-type stars: Weak wind problem

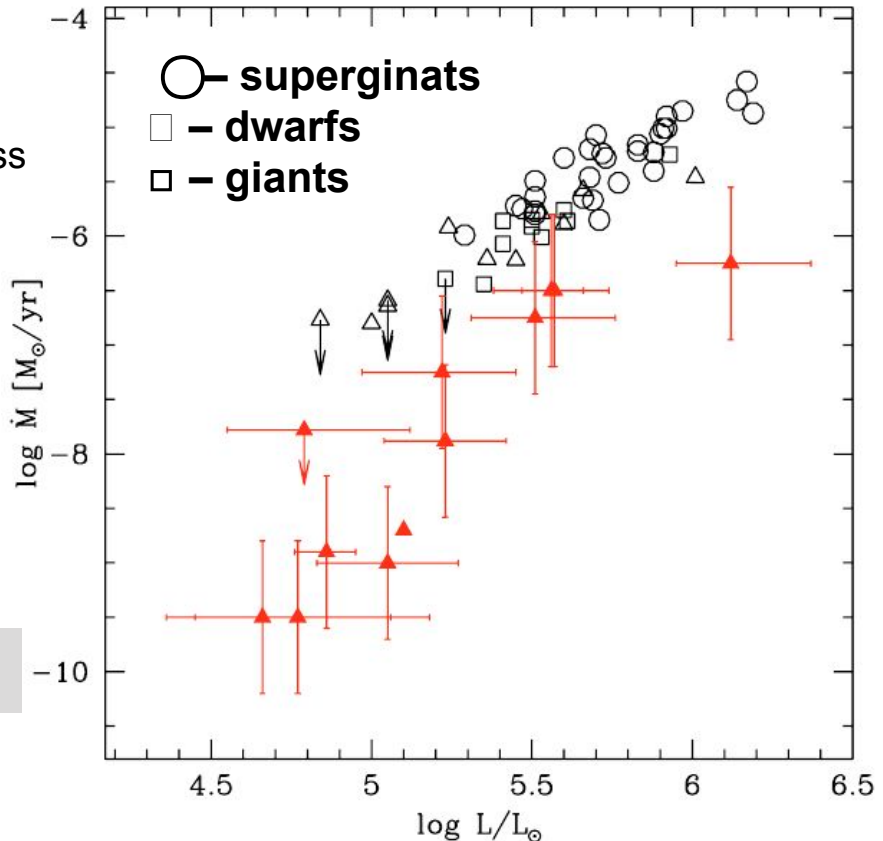
Myr old. Mass loss rates of all stars are found to be lower than expected from the hydrodynamical predictions of Vink et al. (2001).

For stars with $\log L/L_{\odot} \gtrsim 5.2$, the reduction is by less than a factor 5 and is mainly due to the inclusion of clumping in the models.

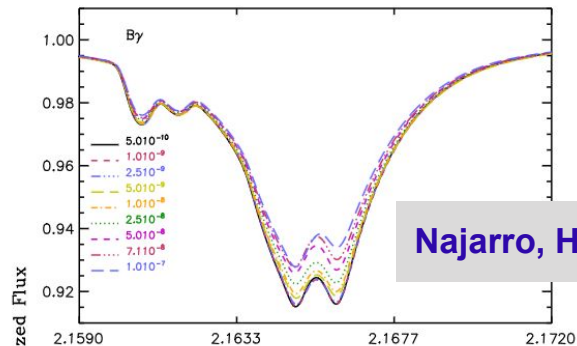
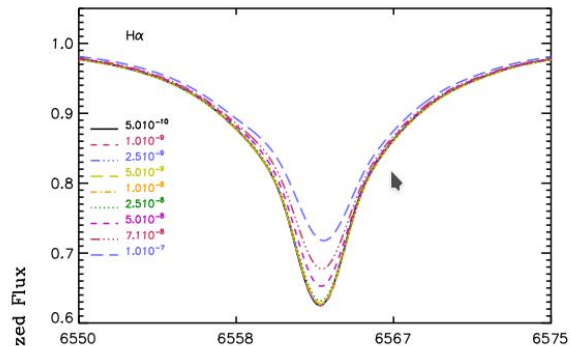
For stars with $\log L/L_{\odot} \lesssim 5.2$ the reduction can be as high as a factor 100

$$\begin{aligned} \log \dot{M} = & -6.697(\pm 0.061) + 2.194(\pm 0.021) \log(L_*/10^5) \\ & -1.313(\pm 0.046) \log(M_*/30) - 1.226(\pm 0.037) \log\left(\frac{v_{\infty}/v_{\text{esc}}}{2}\right) \\ & + 0.933(\pm 0.064) \log(T_{\text{eff}}/40000) - 10.92(\pm 0.90) \{\log(T_{\text{eff}}/40000)\}^2 \end{aligned}$$

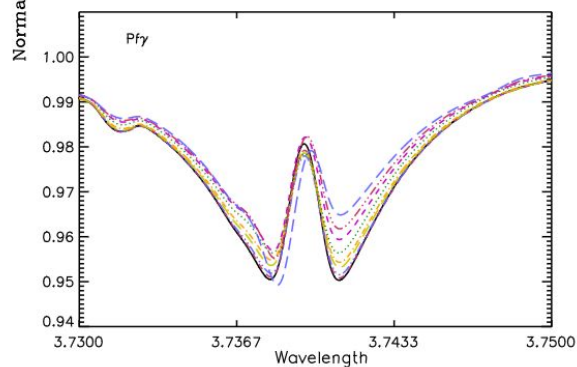
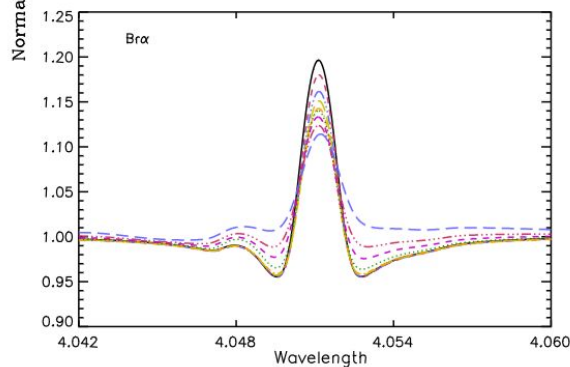
Vink et al. (2001)



CMFGEN application: O-type stars: Weak wind problem



Najarro, Hanson, Puls, 2011

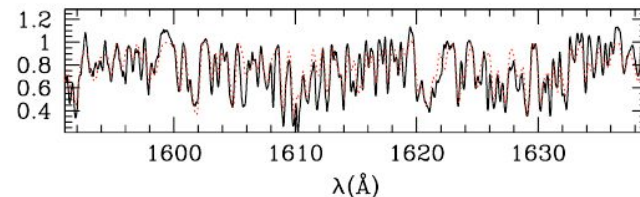
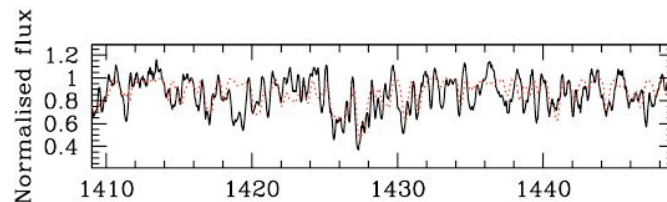
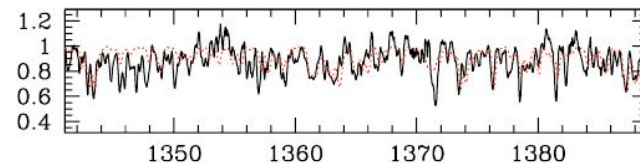


CMFGEN application: O-type stars: X-ray

The inclusion of X-ray emission (possibly due to magnetic mechanisms) in models with low density is crucial to derive accurate mass loss rates from UV lines, while it is found to be unimportant for high density winds.

Martins et al. 2005 “O stars with weak winds: the Galactic case”

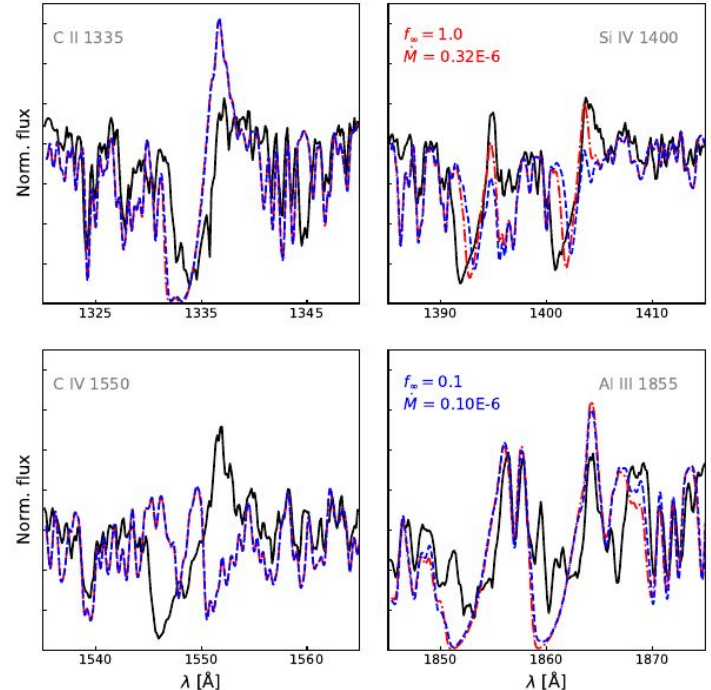
CMFGEN allows the possibility to include X-ray emission in the models. Practically, as X-rays are thought to be emitted by shocks distributed in the wind, two parameters are adopted to take them into account: one is a shock temperature (chosen to be 3×10^6 K since it is typical of high energy photons in O type stars) to set the wavelength of maximum emission, and the other is a volume filling factor which is used to set the level of emission.



CMFGEN application: B-type stars: X-ray

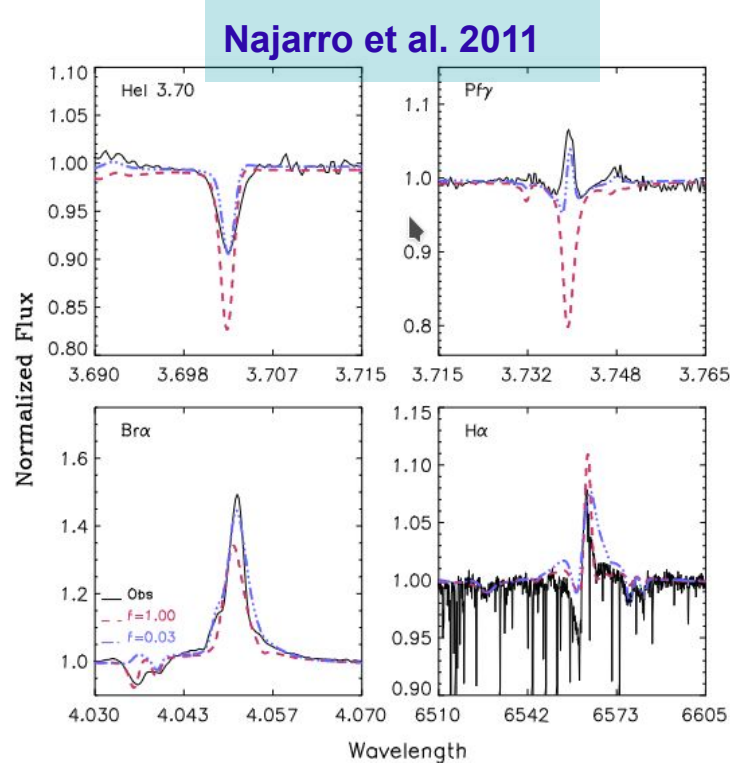
Bernini-Peron et al. 2023, “Clumping and X-Rays in cooler B supergiant stars”

When including both clumping and X-rays, we obtained a good agreement between synthetic and observed spectra for our sample stars. **For the first time, we reproduced key wind lines in the UV, where previous studies were unsuccessful.** To model the UV spectra, we require a moderately clumped wind ($fV^\infty \gtrsim 0.5$). We also infer a relative X-ray luminosity of about $10^{-7.5}$ to 10^{-8} , which is lower than the typical ratio of 10^{-7} . Moreover, we find a possible mismatch between evolutionary mass predictions and the derived spectroscopic masses, which deserves deeper investigation as this might relate to the mass-discrepancy problem present in other types of OB stars.



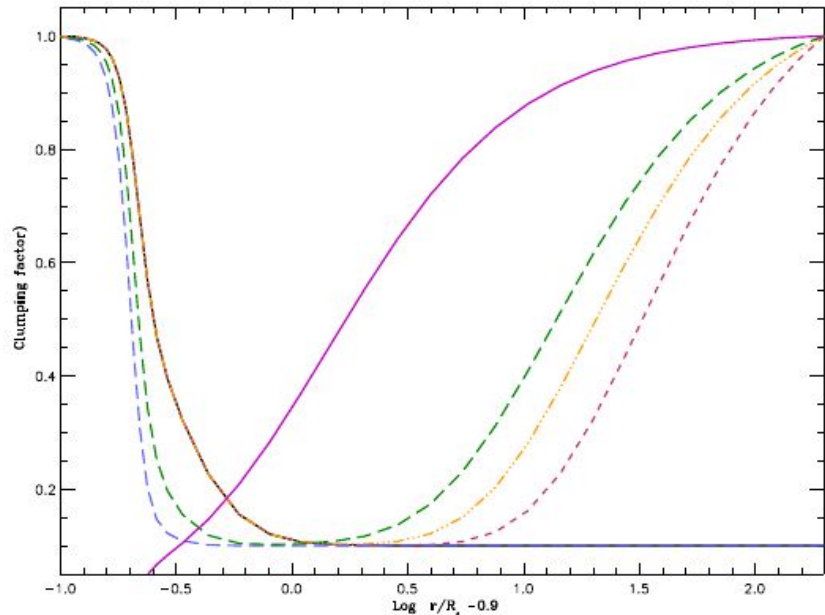
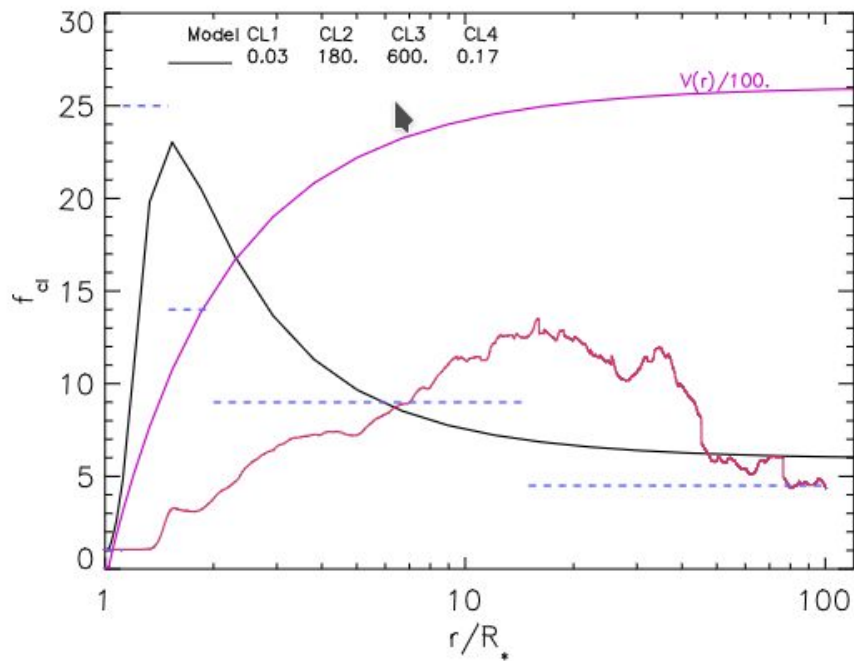
Clumping

For objects with dense winds, Br α samples the intermediate wind while P γ maps the inner one. In combination with other indicators (UV, H α , Br γ) these lines enable us to constrain the wind clumping structure and to obtain "true" mass-loss rates. For objects with weak winds, Br α emerges as a reliable diagnostic tool to constrain \dot{M} . The emission component at the line Doppler-core superimposed on the rather shallow Stark absorption wings reacts very sensitively to mass loss already at very low \dot{M} values. On the other hand, the line wings display similar sensitivity to mass loss as H α , the classical optical mass loss diagnostics. L-band might be used for estimations clumping properties and mass-loss rates of hot star winds. Br α will become the primary diagnostic tool to measure very low mass-loss rates with unprecedented accuracy.



Clumping

$$f = CL_1 + (1 - CL_1)e^{\frac{-V}{CL_2}} + (CL_4 - CL_1)e^{\frac{(V - V_\infty)}{CL_3}}$$

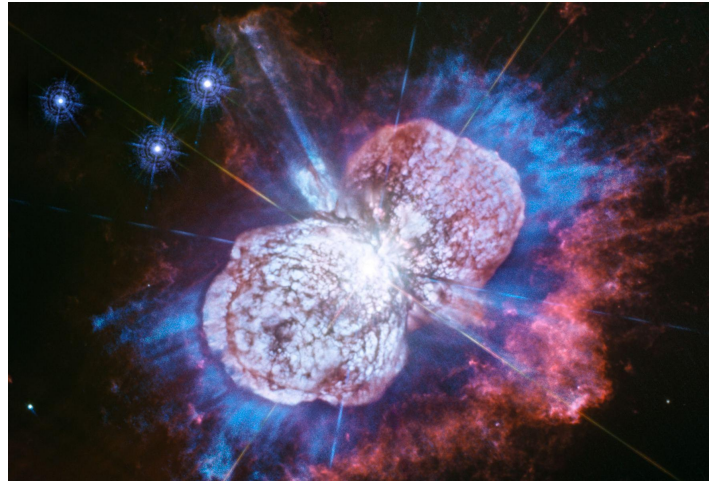


CMFGEN application: Luminous Blue Variables

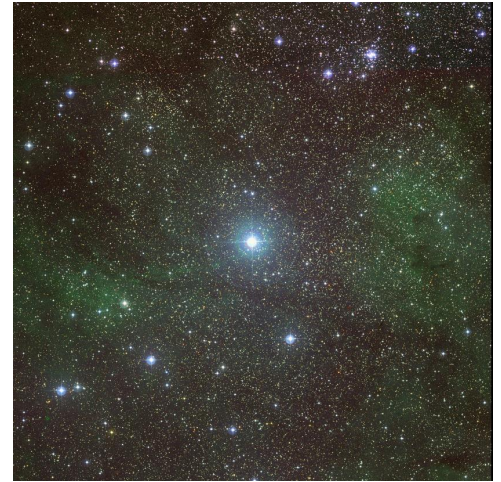
CMFGEN was used for modeling all famous LBVs



AG Car



η Car



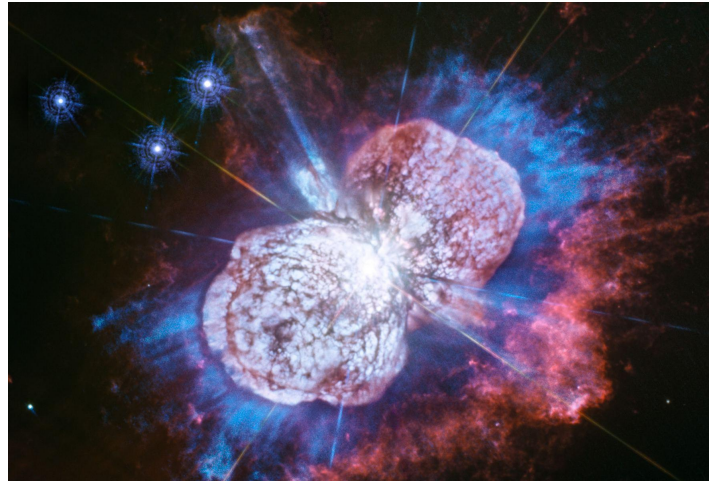
P Cyg

CMFGEN application: Luminous Blue Variables

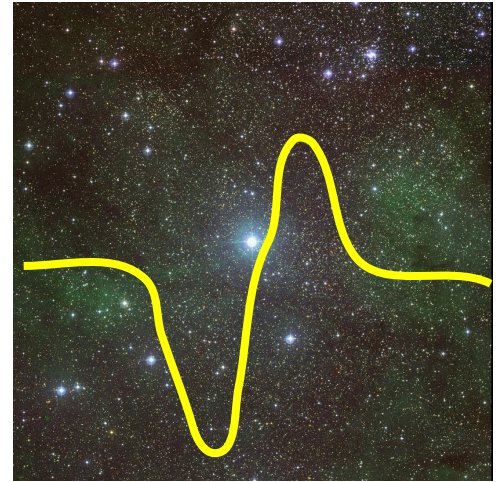
CMFGEN was used for modeling all famous LBVs



AG Car



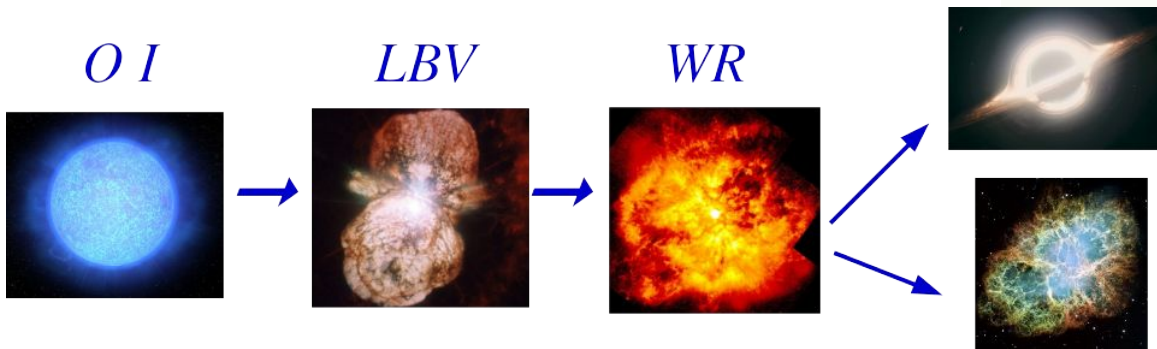
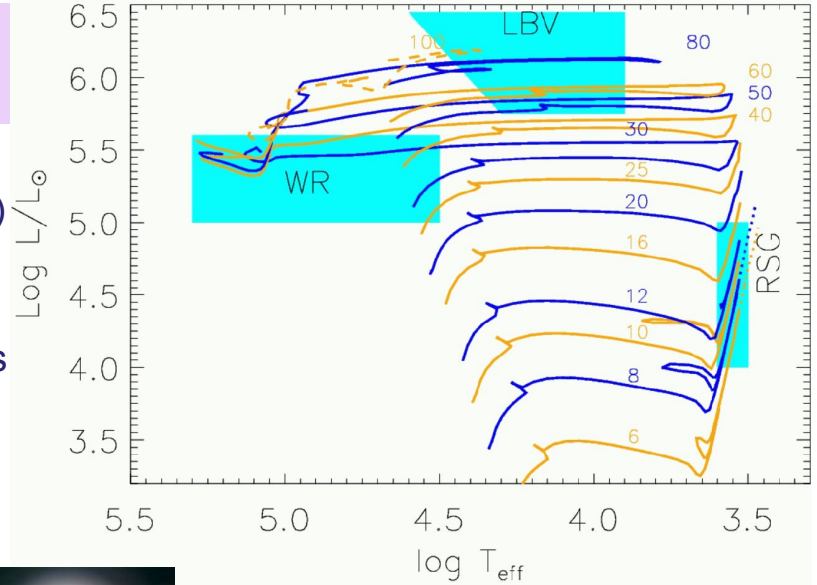
η Car



P Cyg

Luminous Blue Variables

- **Photometric variability** Short (0.1-0.5 mag)
S Dor cycles (1-2 mag)
Giant eruption
- **Spectral variability** from B supergiants or late
Of/WN stars to A-supergiants
- **Bolometric magnitude** $-9.7 > M_{\text{bol}} > -11.5$



CMFGEN application: LBV – P Cygni

Najarro, 2000 “Spectroscopy of P Cygni” → UV, optical, IR

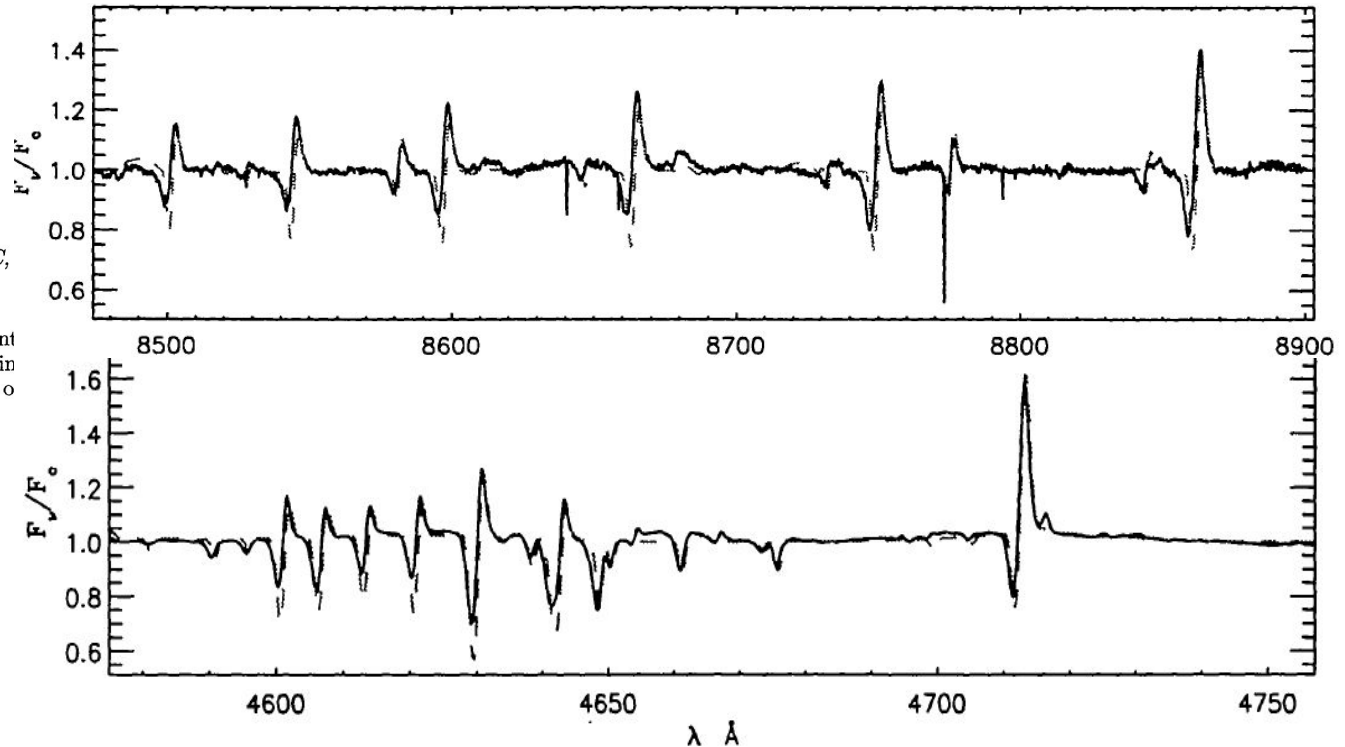
P CYGNI 2000; 400 YEARS OF PROGRESS
ASP Conference Series, Vol. 233, 2001
Mart de Groot & Christiaan Sterken, eds.

Spectroscopy of P Cygni

F. Najarro

Instituto de Estructura de la Materia, CSIC,
Madrid, Spain

Abstract. We present a full UV to IR quant
sis of P Cygni using a new generation of lin
tended atmospheres with stellar winds. The o



CMFGEN application: LBV – P Cygni

Najarro, 2000 “Spectroscopy of P Cygni” → UV, optical, IR

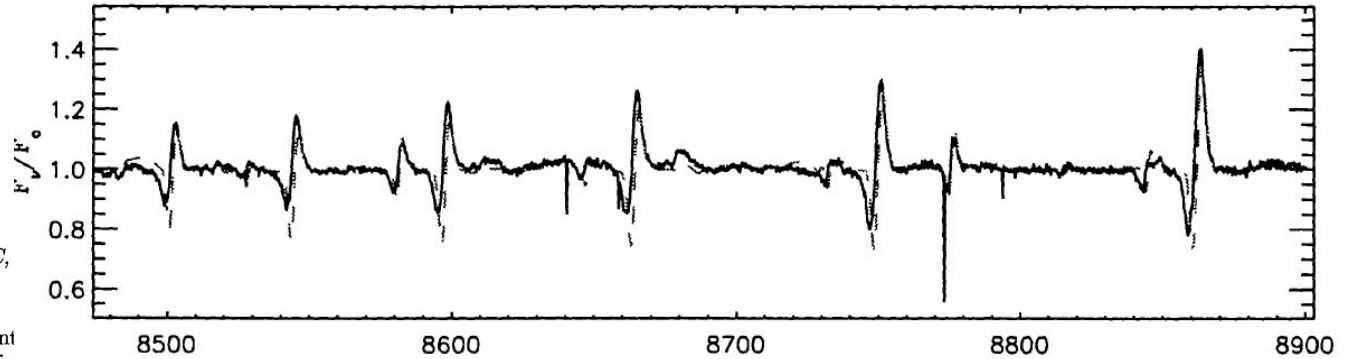
P CYGNI 2000; 400 YEARS OF PROGRESS
ASP Conference Series, Vol. 233, 2001
Mart de Groot & Christiaan Sterken, eds.

Spectroscopy of P Cygni

F. Najarro

Instituto de Estructura de la Materia, CSIC,
Madrid, Spain

Abstract. We present a full UV to IR quant
sis of P Cygni using a new generation of lin
tended atmospheres with stellar winds. The o



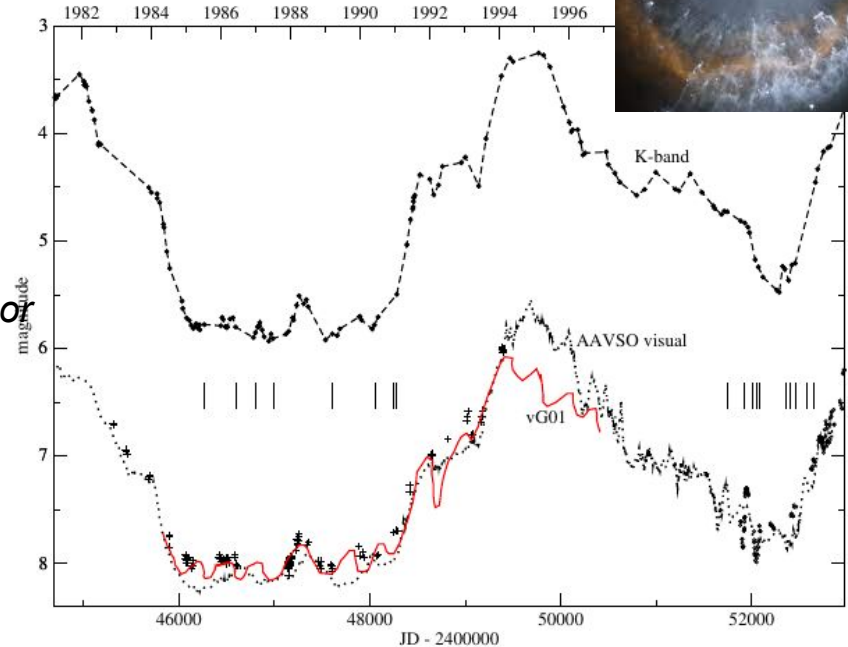
Model	R_* (R_\odot)	L_* (L_\odot)	T_{eff} (10^4K)	$n_{\text{He}}/n_{\text{H}}$	$\dot{M}/f^{1/2}$ ($M_\odot \text{ yr}^{-1}$)	v_∞ (km s^{-1})	β
Optical	76	7.0×10^5	1.92	.29	3.2×10^{-5}	185	4.5
ISO-SWS	76	5.6×10^5	1.81	.30	3.0×10^{-5}	185	2.5
Blanketed	76	6.1×10^5	1.87	.29	3.3×10^{-5}	185	2.5

CMFGEN application: Luminous Blue Variables

CMFGEN allows to estimate luminosity of star, that makes CMFGEN important tool for studies of luminous blues variables (LBV)

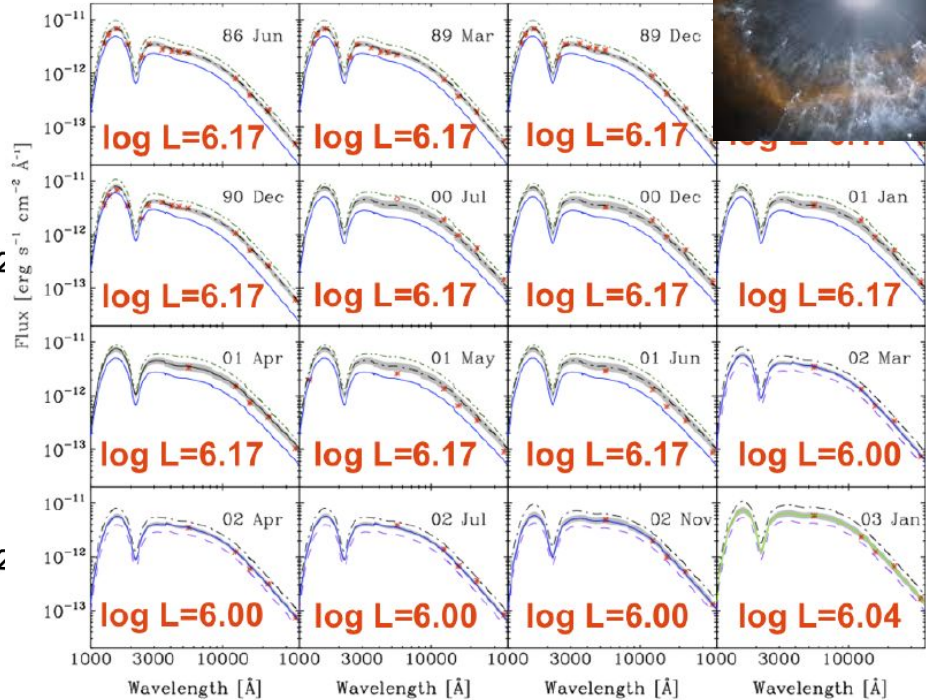
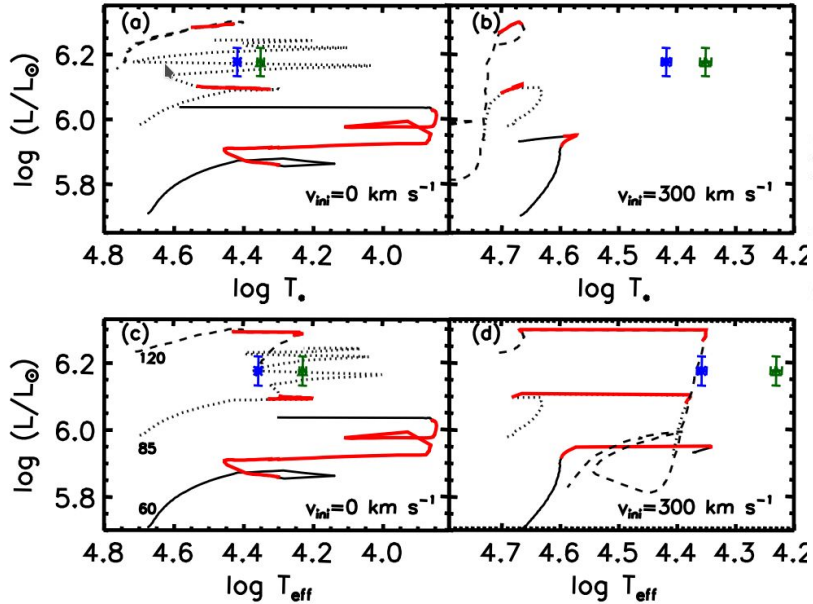
Groh et al., 2009 “*On the Nature of the Prototype Luminous Blue Variable Ag Carinae. I. Fundamental Parameters During Visual Minimum Phases and Changes in the Bolometric Luminosity During the S-Dor Cycle*”

Groh, Hillier, Daminieli, 2011 “*On the Nature of the Prototype Luminous Blue Variable AG Carinae. II. Witnessing a Massive Star Evolving Close to the Eddington and Bistability Limits*”



LBV star AG Carinae (AG Car) is one of the most luminous stars in the Milky Way

CMFGEN application: Luminous Blue Variables



Groh et al., 2009, 2011

CMFGEN application: Luminous Blue Variables



Minimum phases of AG Car are not equal to each other
 maximum effective temperature
 1985–1990 → 22, 800 K; 2000–2001 → 17, 000 K

Significantly different effective temperatures achieved by AG Car during the consecutive visual minima of 1985–1990 ($T_{\text{eff}} 22,800 \text{ K}$) and 2000–2001 ($T_{\text{eff}} 17,000 \text{ K}$) place the star on different sides of the bistability limit, which occurs in line-driven stellar winds around $T_{\text{eff}} \sim 21,000 \text{ K}$.

Epoch	V^a	BC (mag)	$\log(L_*/L_\odot)^b$ (mag)	R_* (R_\odot)	R_{phot} (R_\odot)	T_* (K)	T_{eff} (K)	\dot{M} ($M_\odot \text{ yr}^{-1}$)	v_∞ (km s^{-1})	f
1985 Jul – 1986 Jun	7.98	-2.50	6.17	58.5	78.7	26,450	22,800	1.9×10^{-5}	300	0.10
1987 Jan – 1990 Jun	8.00	-2.52	6.17	59.6	78.7	26,200	22,800	1.5×10^{-5}	300	0.10
1990 Dec – 1991 Jan	7.71	-2.23	6.17	67.4	88.5	24,640	21,500	1.5×10^{-5}	300	0.10
2000 Jul–2001 Jun	7.63	-2.15	6.17	85.3	141.6	21,900	17,000	3.7×10^{-5}	105	0.15
2002 Mar–2002 Jul	7.60	-1.68	6.00	95.5	124.2	18,700	16,400	4.7×10^{-5}	195	0.25
2002 Nov	7.20	-1.28	6.00	120.4	170.4	16,650	14,000	6.0×10^{-5}	200	0.25
2003 Jan	7.03	-1.22	6.04	115.2	171.3	17,420	14,300	6.0×10^{-5}	150	0.25

CMFGEN application: [WR] stars

“Wolf-Rayet” is really an astrophysical phenomenon of fast-moving, hot plasma, normally expanding around a hot star.

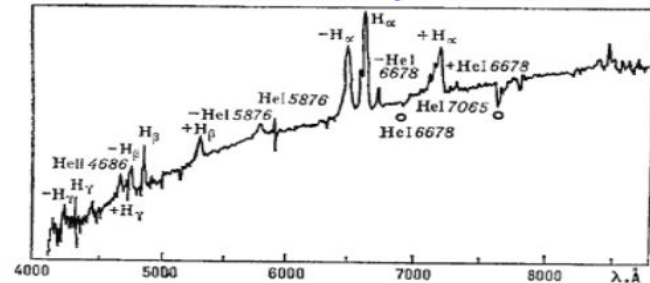
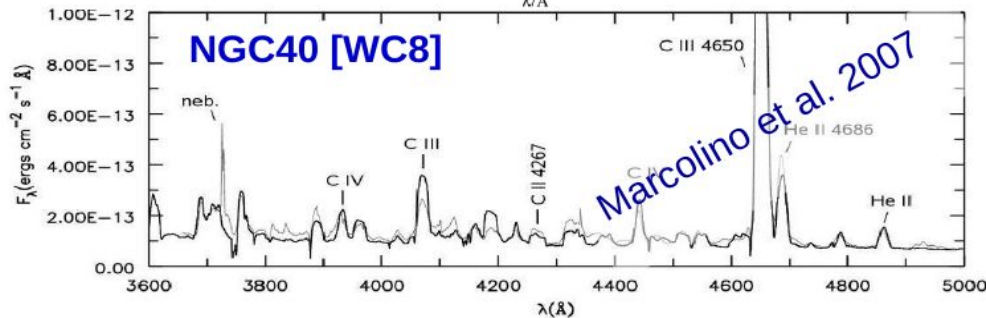
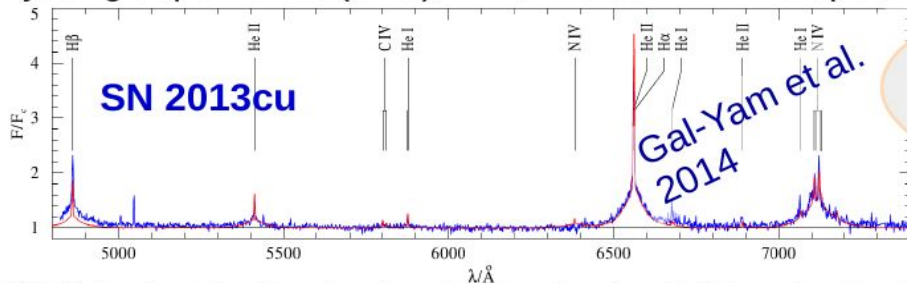
We may observe WR phenomen in:

- ▶ “classical” WR stars – descendants of massive ($M > 25M_{\odot}$) O-type stars
- ▶ very massive stars (VMS) with $M > 100M_{\odot}$
- ▶ [WR] central stars of planetary nebula (CSPN)
- ▶ young supernovae (SNe), which reveal WR-like spectra

Eddington factor Γ_e – key to the WR phenomenon

$$\Gamma_e = g_{\text{rad}}^{\text{elec}} / g_{\text{grav}} = \sigma_{\text{elec}} L / (4\pi c G M)$$

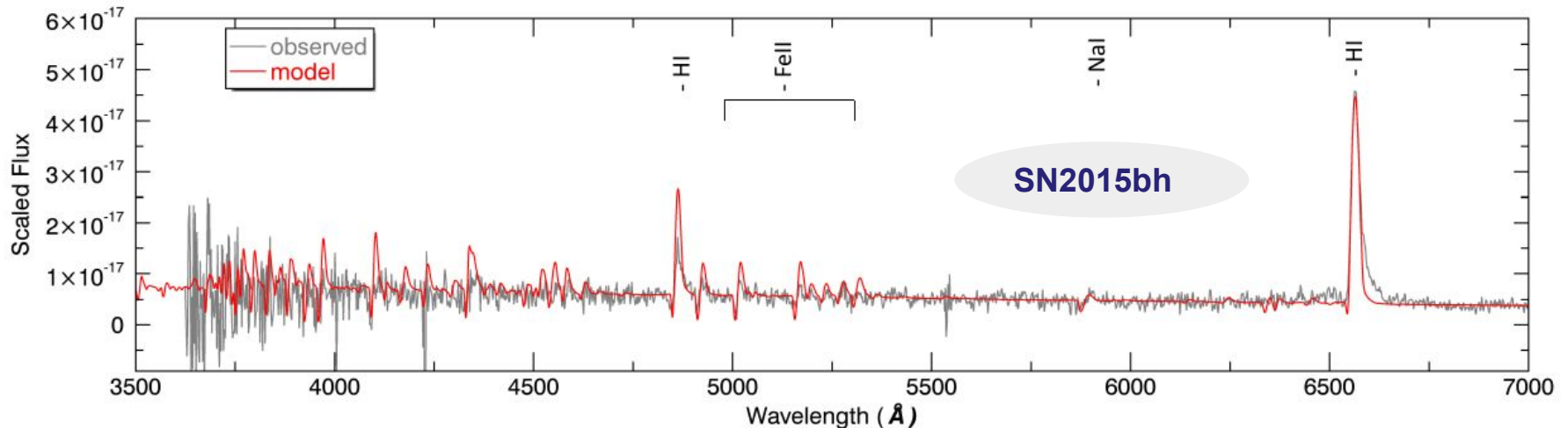
!!! Moreover – optical spectrum of Galactic microquasar SS433



CMFGEN application: pre-Supernova

CMFGEN modeling show that progenitor of SN2015bh had an T_{eff} between 8700 and 10000 K, luminosity $\approx 2.7 \times 10^6 L_{\odot}$, contained at least 25% H in mass at the surface, and half-solar Fe abundances. The results

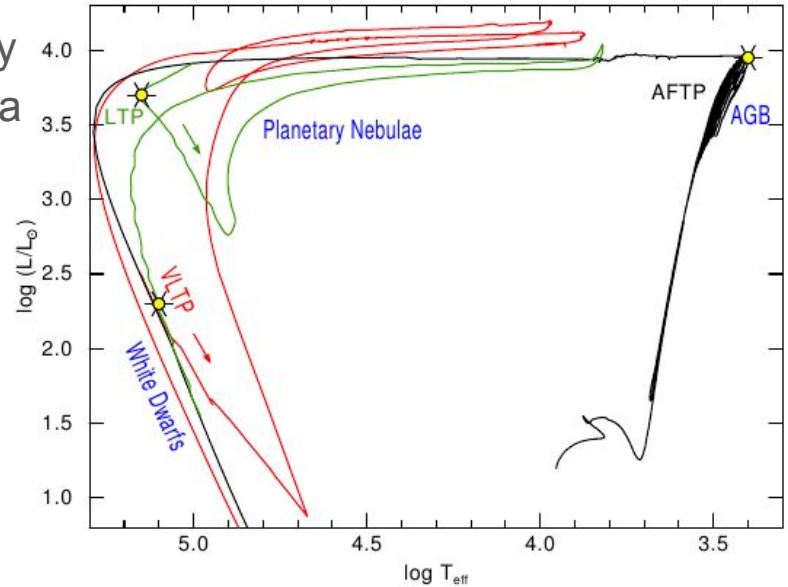
Boian & Groh, 2017, “*Catching a star before explosion: the luminous blue variable progenitor of SN2015bh*”



Flux-calibrated spectrum of SN2015bh observed on 12 November 2013. The model has been scaled to a distance of $d = 27$ Mpc and reddened using $E(B-V) = 0.25$ and $RV = 3.1$

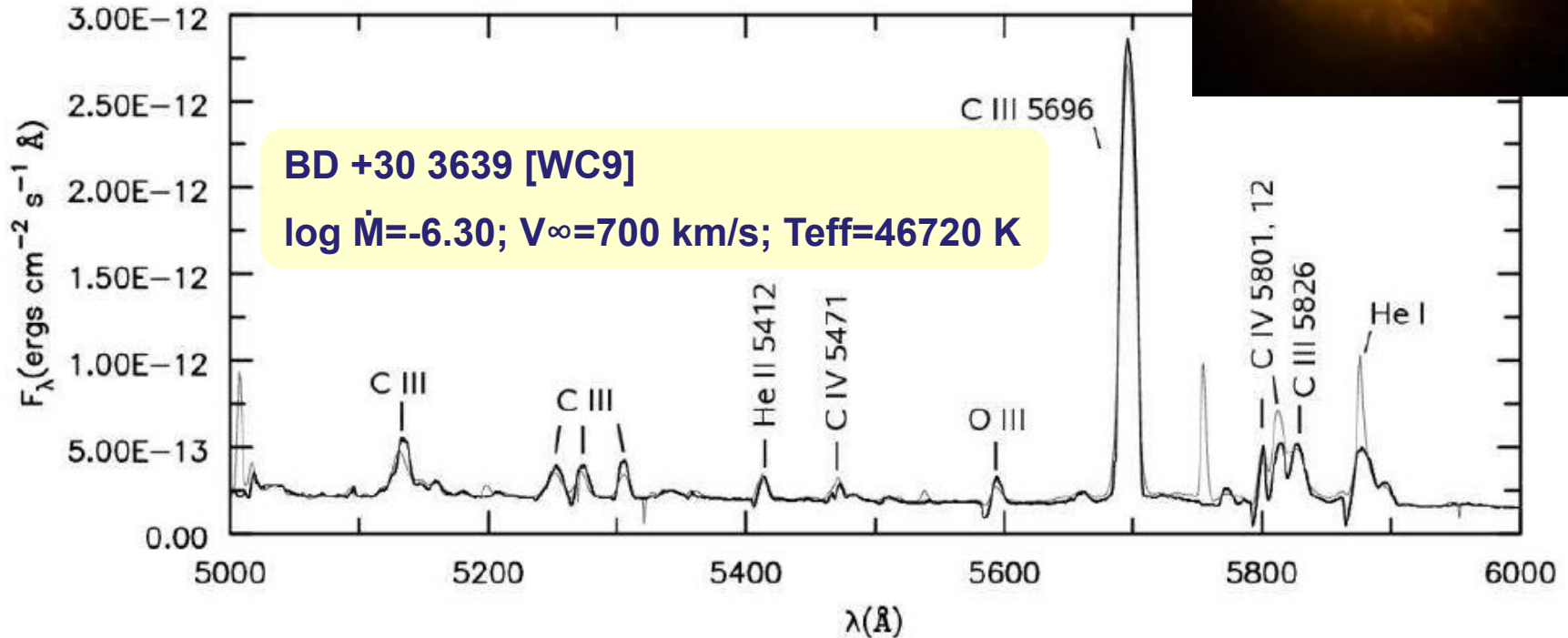
CMFGEN application: [WR] stars

A significant number of the central stars of planetary nebulae (CSPNe) are hydrogen-deficient, showing a chemical composition of helium, carbon, and oxygen. Most of them exhibit Wolf–Rayet-like emission line spectra, similar to those of the massive WC Pop I stars, and are therefore classified as of spectral type [WC] or [WO].



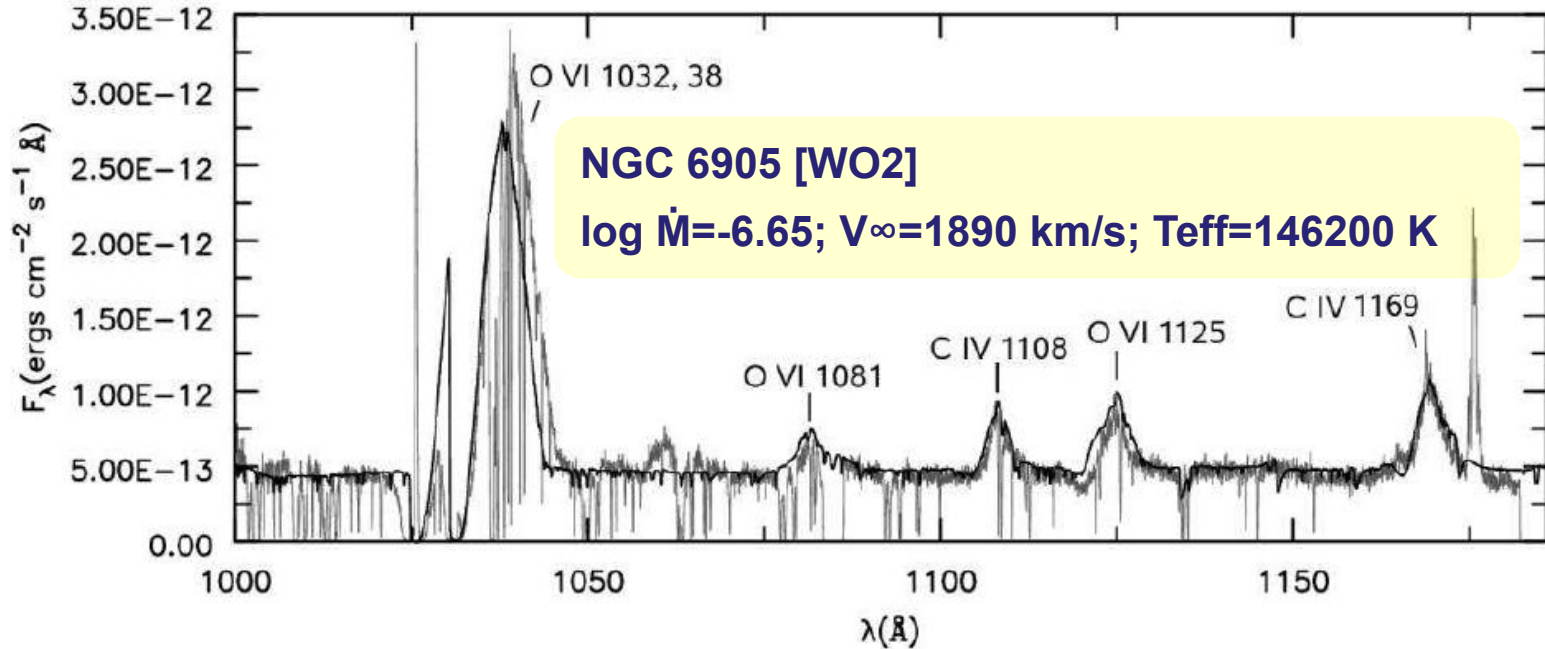
CMFGEN application: [WR] stars

Marcolino et al. 2007, "Detailed far-ultraviolet to optical analysis of four [WR] stars"



CMFGEN application: [WR] stars

Marcolino et al. 2007, “Detailed far-ultraviolet to optical analysis of four [WR] stars”



CMFGEN application: [WR] stars

Star	T_* (K)	R_*/R_\odot	T_{eff} (K)	$\log \dot{M}$	$\log \dot{M}/\sqrt{f}$	v_∞ (km s ⁻¹)	R_T/R_\odot	β_{He}	β_{C}	β_{O}	d (kpc)
BD +30 3639 (this work).....	48060	1.0	46720	-6.30	-5.80	700	6.8 (14.6)	43	51	6	1.2
Leuenhagen et al. (1996).....	47000	1.49	42000	...	-5.40	700	5.5 (...)	45	50	5	...
Crowther et al. (2006).....	55000	0.85	48000	-6.05	-5.55	700	3.9 (8.5)	51	38	10	...
NGC 40 (this work).....	73310	0.43	70840	-6.25	-5.75	1000	3.4 (7.4)	43	51	6	1.4
Leuenhagen et al. (1996).....	78000	0.46	46000	...	-5.40	1000	2.2 (...)	40	50	10	...
NGC 5315 (this work).....	76420	0.40	74590	-6.33	-5.83	2400	6.5 (13.9)	43	51	6	2.5
de Freitas Pacheco et al. (1986, 1993).....	82700	0.31	-5.83	2600	5.2 (...)
NGC 6905 (this work).....	149600	0.10	146200	-7.15	-6.65	1890	4.9 (10.5)	49	40	10	1.75
Koesterke & Hamann (1997b).....	141000	1800	3.4 (...)	60	25	15	...

CMFGEN application: Supernova

SN 1994W: an interacting supernova or two interacting shells?

Luc Dessart, D. John Hillier, Suvi Gezari, Stephane Basa, and Tom Matheson, 2009, MNRAS, 394, 21. Click [here](#) for the results and model spectra.

Type II-Plateau supernova radiation: dependences on progenitor and explosion properties

Luc Dessart, D. John Hillier, Roni Waldman, and Eli Livne, 2013, MNRAS, 433, 1745. Click [here](#) to the results and models.

Radiative properties of pair-instability supernova explosions

Dessart, Luc Waldman, Roni; Livne, Eli; Hillier, D. John; Blondin, Stephane, 2013, MNRAS, 428, 3227. Click [here](#) for the results and models.

One-dimensional delayed-detonation models of Type Ia supernovae: Confrontation to observations at bolometric maximum

Stéphane Blondin, Luc Dessart, D. John Hillier, and Alexei M. Khokhlov, 2013, MNRAS, 429, 2127. Click [here](#) for the results and models.

Constraints on the explosion mechanism and progenitors of Type Ia supernovae

Luc Dessart, Stéphane Blondin, D. John Hillier, and Alexei M. Khokhlov, 2014, MNRAS, 441, 532 Click [here](#) for the results, models etc.

Critical ingredients of Type Ia supernova radiative-transfer modelling

Luc Dessart, D. John Hillier, Stéphane Blondin, and Alexei M. Khokhlov, 2014, MNRAS, 441, 3249. Click [here](#) for the results, models etc.

[Co III] versus Na I D in Type Ia supernova spectra

Luc Dessart, D. John Hillier, Stéphane Blondin, and Alexei M. Khokhlov, 2014, MNRAS, 439, 3114. Click [here](#) for the results, models etc.

A one-dimensional Chandrasekhar-mass delayed-detonation model for the broad-lined Type Ia supernova 2002bo

Stéphane Blondin, Luc Dessart, and D. John Hillier, 2015, MNRAS, 448, 2766. Click [here](#) for the results and models.

One-dimensional non-LTE time-dependent radiative transfer of an He-detonation model and the connection to faint and fast-decaying supernovae

Dessart, Luc, and Hillier, D. John; 2015, MNRAS, 447, 1370. Click [here](#) for the results and models.

Numerical simulations of superluminous supernovae of type IIn

Luc Dessart, Edouard Audit, and D. John Hillier, 2015, MNRAS, 449, 4304. Click [here](#) for the results and model spectra.

Luc Dessart

CMFGEN application: Supernova

The detonation of a sub-Chandrasekhar-mass white dwarf at the origin of the low-luminosity Type Ia supernova 1999by

Stephane Blondin, Luc Dessart, and D. John Hillier, 2017, MNRAS, 474, 3931. Click [here](#) for the results and models.

Explosion of red-supergiant stars: Influence of the atmospheric structure on shock breakout and early-time supernova radiation

Luc Dessart, D. John Hillier, and Edouard Audit, 2017, A&A, 605, 83. Click [here](#) for the results and models.

A study of the low-luminosity Type II-Plateau SN 2008bk

Sergey Lisakov, Luc Dessart, D. John Hillier, Roni Waldman, and Eli Livne, 2017, MNRAS, 466, 33. Click [here](#) to the results and models.

A magnetar model for the hydrogen-rich super-luminous supernova iPTF14hls.

Luc Dessart, 2018, A&A, 610, 10. Click [here](#) for the results and models.

Supernovae from blue supergiant progenitors: What a mess!

Luc Dessart and D. John Hillier, 2019, A&A, 622, 70. Click [here](#) for the results and models.

Simulations of light curves and spectra for superluminous Type Ic supernovae powered by magnetars

Luc Dessart, 2019, A&A, 621, 141. Click [here](#) for the results and models.

The explosion of 9-29Msun stars as Type II supernovae: Results from radiative-transfer modeling at one year after explosion.

Dessart, Luc, Hillier, D. John, Sukhbold, Tuguldur, Woosley, Stan, and Janka, H.-T. 2021, A&A, 652, 64 Click [here](#) for the results and models.

Nebular phase properties of supernova Ibc from He-star explosions

Dessart, Luc, Hillier, D. John, Sukhbold, Tuguldur, Woosley, Stan, and Janka, H.-T. 2021, accepted for publication in A&A Click [here](#) for the results and models.

CMFGEN application: Supernova

Dessart & Hillier (2005)

presented first results on the quantitative spectroscopic analysis of photospheric-phase of type II supernovae (SN).

The model parameters are:

$$L_* = 1.5 \times 10^8 L_{\odot};$$

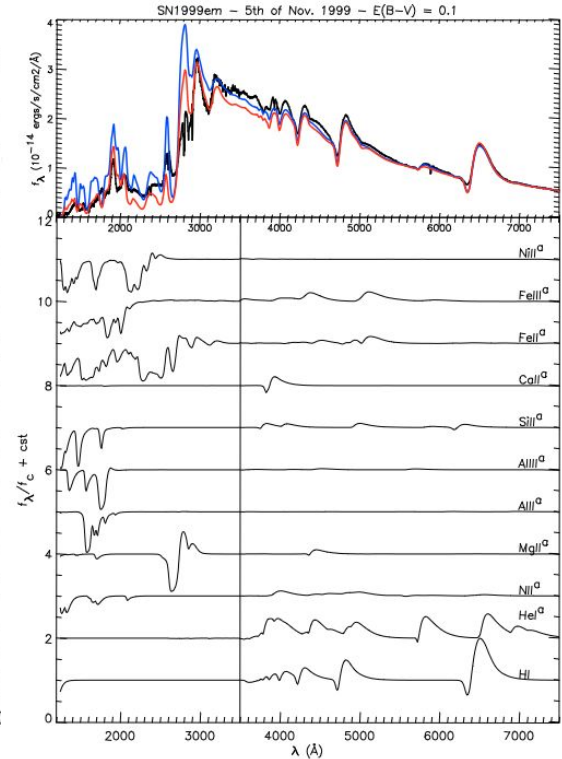
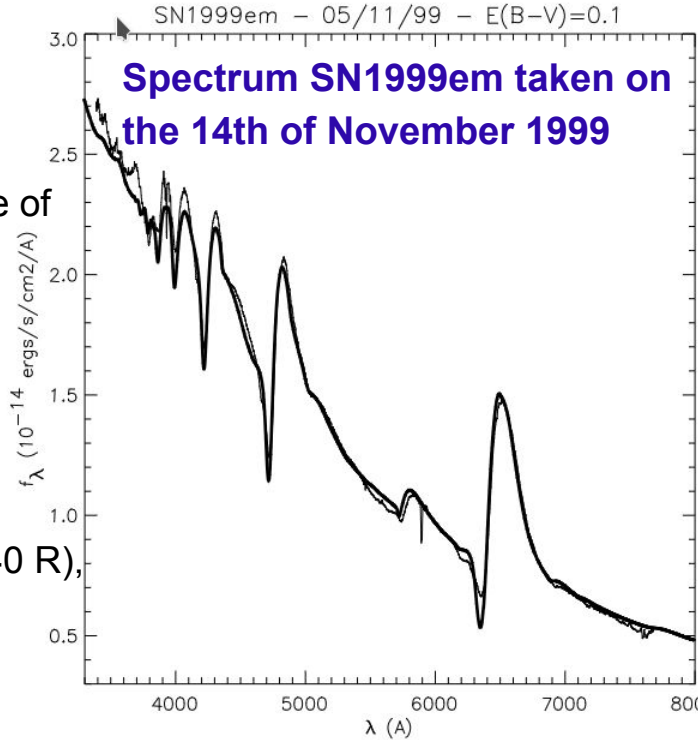
$$R_{\text{phot}} = 6.15 \times 10^{14} \text{ cm (or 8840 R)},$$

$$v_{\text{phot}} = 6350 \text{ km s}^{-1};$$

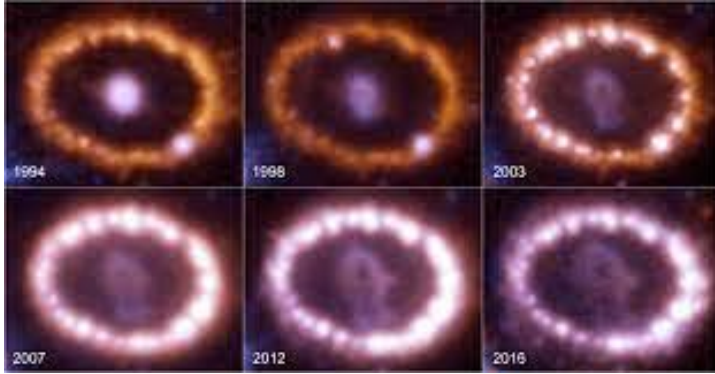
$$T_{\text{eff}} = 6800 \text{ K};$$

$$n = 10;$$

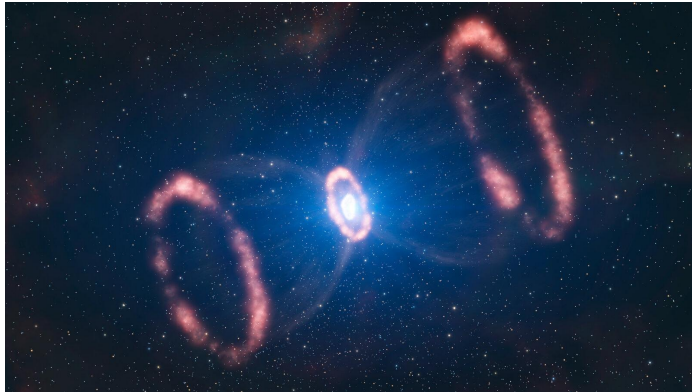
$$\rho_{\text{phot}} = 8.7 \times 10^{-14} \text{ g cm}^{-3}$$



CMFGEN application: Supernova

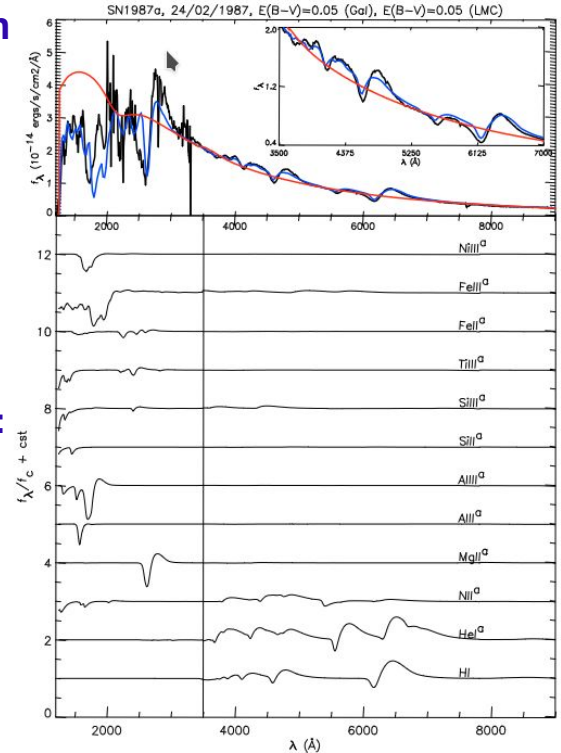


Spectrum SN1987A taken on the February 24 1987



The model parameters are:

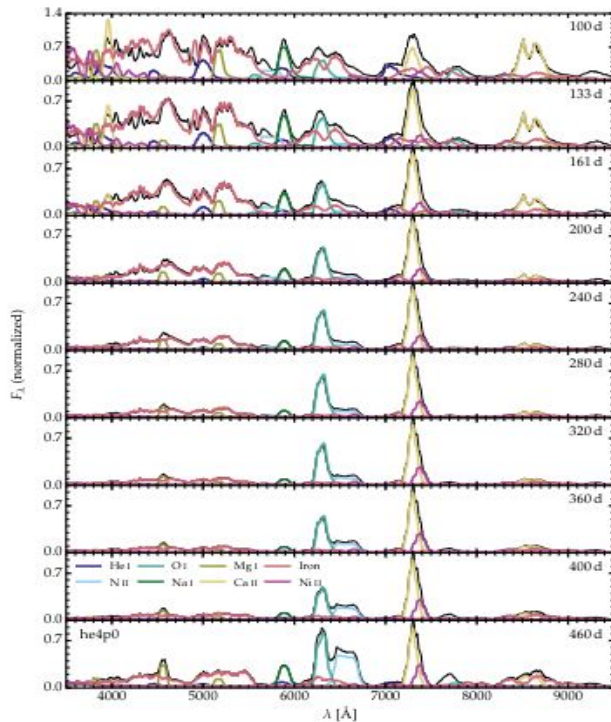
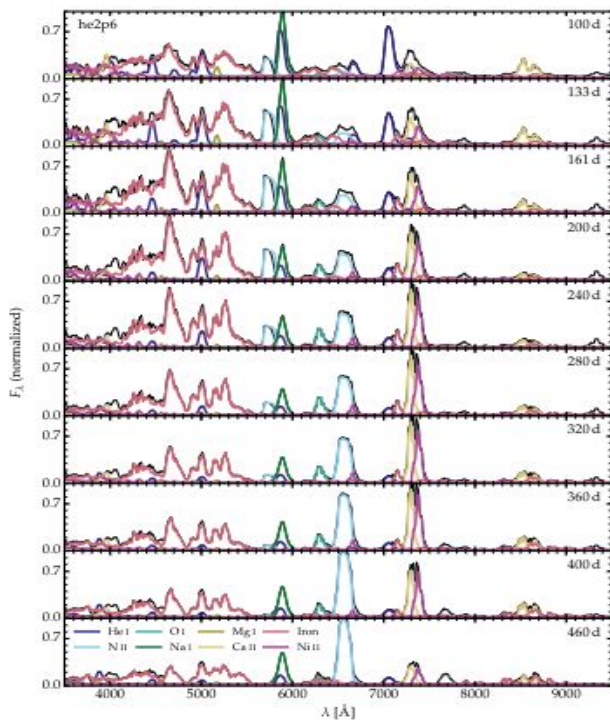
- $L_* = 3 \times 10^8 L_{\odot}$;
- $R_{\text{phot}} = 2.74 \times 10^{14} \text{ cm}$
(or 3940 R);
- $v_{\text{phot}} = 17700 \text{ km s}^{-1}$;
- $T_{\text{eff}} = 11200 \text{ K}$;
- $n = 12$;
- $\rho_{\text{phot}} = 1.1 \times 10^{-13} \text{ g cm}^{-3}$



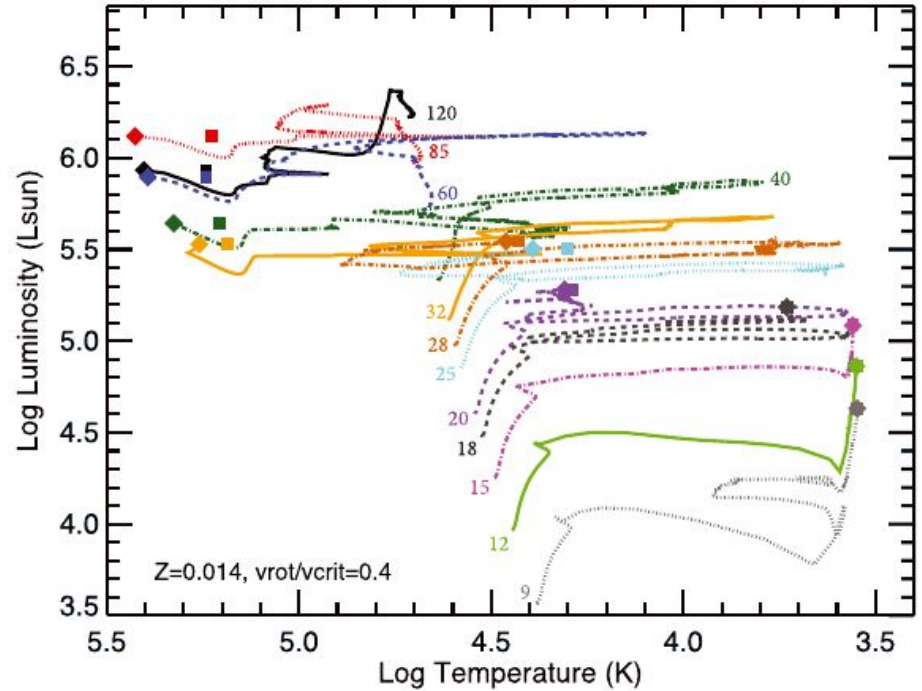
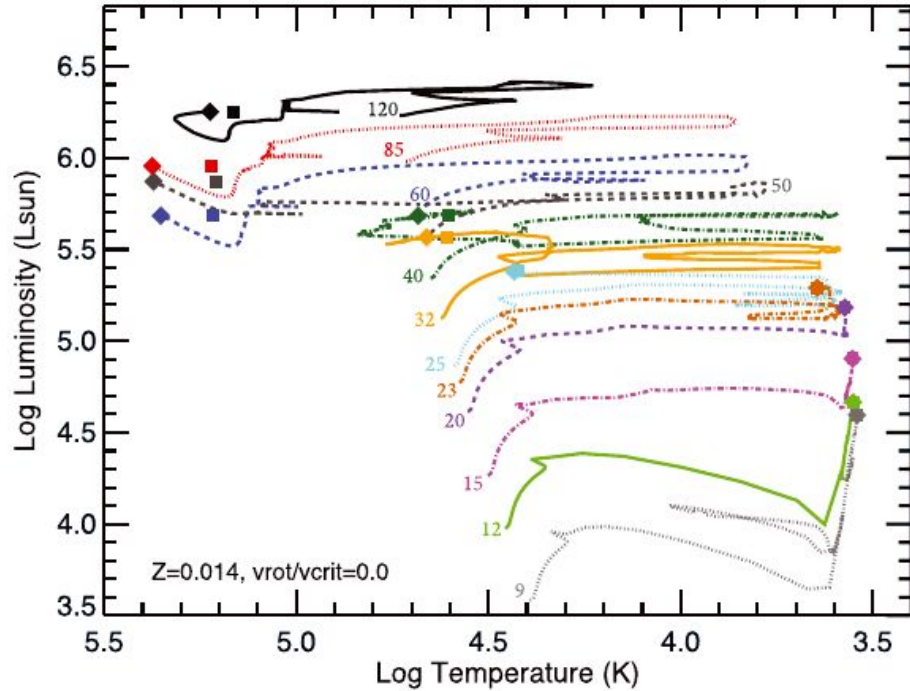
CMFGEN application: Supernova

Dessart et al., 2023 “Modeling of the nebular-phase spectral evolution of stripped-envelope supernovae. New grids from 100 to 450 days”

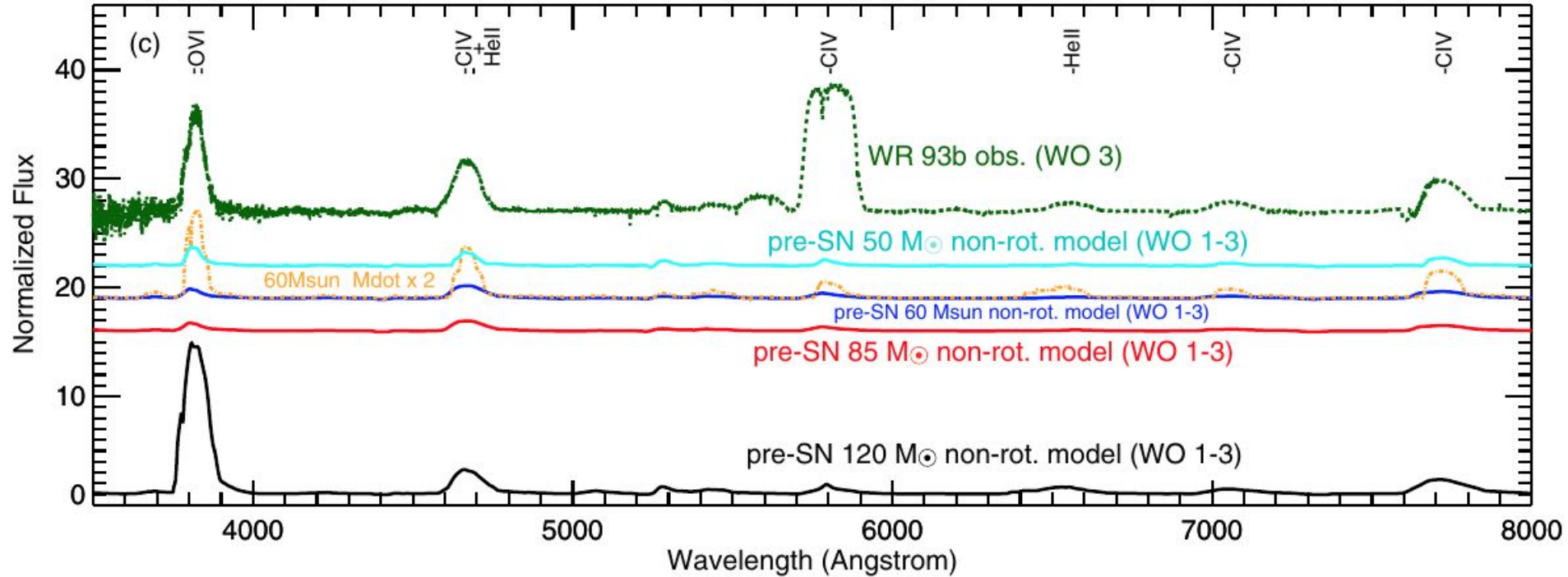
Dessart et al. 2023 presented extended grid of multi-epoch 1D nonlocal thermodynamic equilibrium radiative transfer calculations for nebular-phase Type Ibc SNe from He-star explosions. Spectral evolution from 100 to about 450 days was studied.



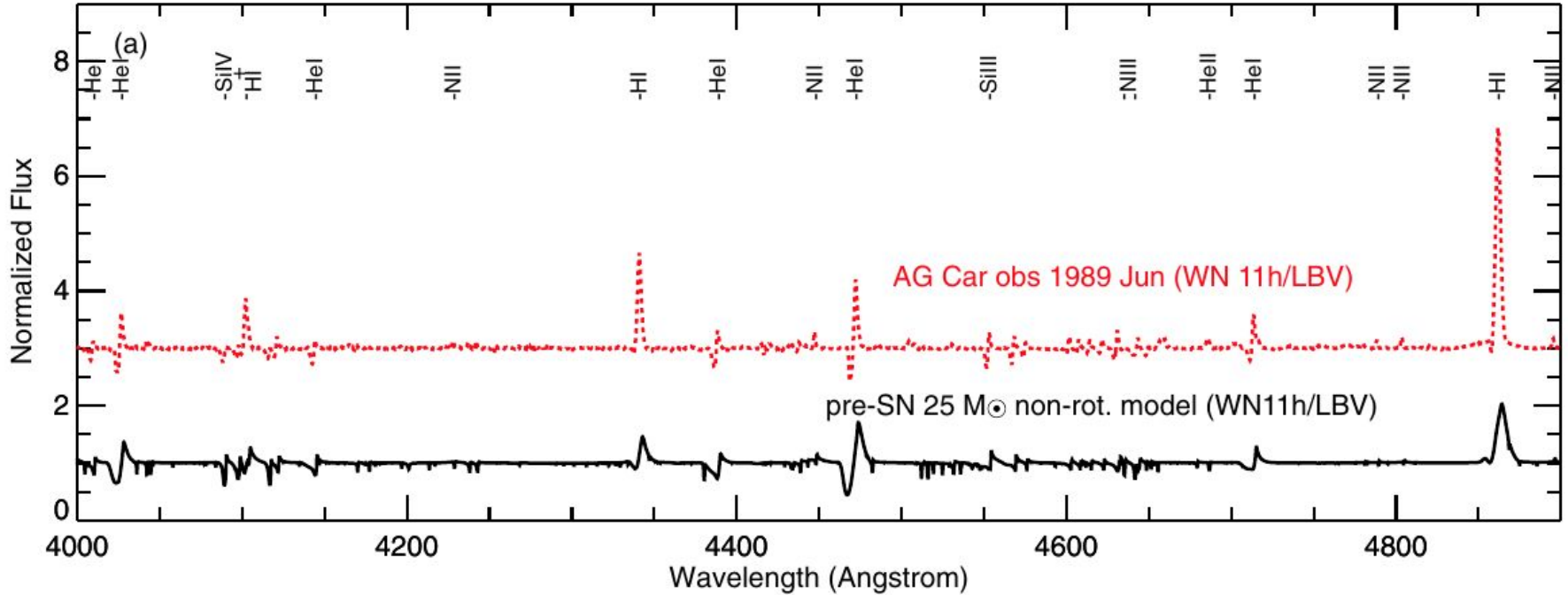
CMFGEN and Evolutionary Codes



CMFGEN and Evolutionary Codes

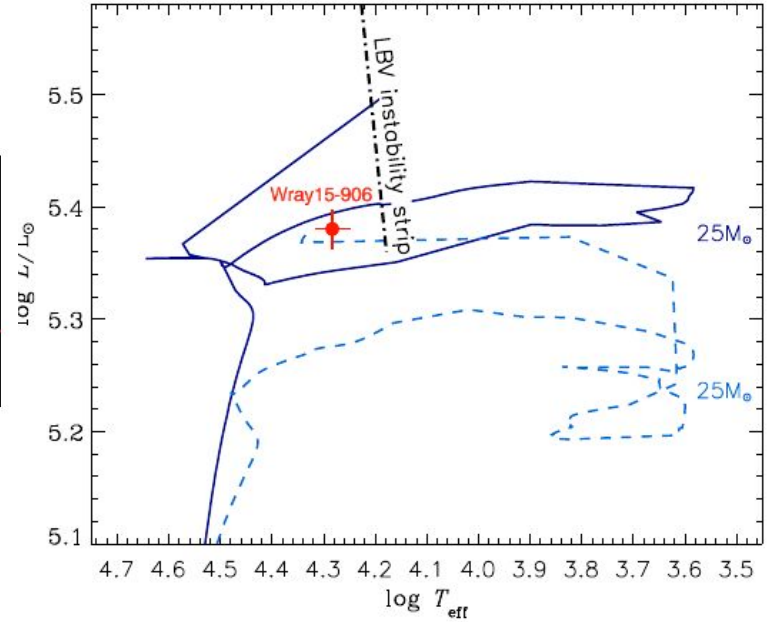
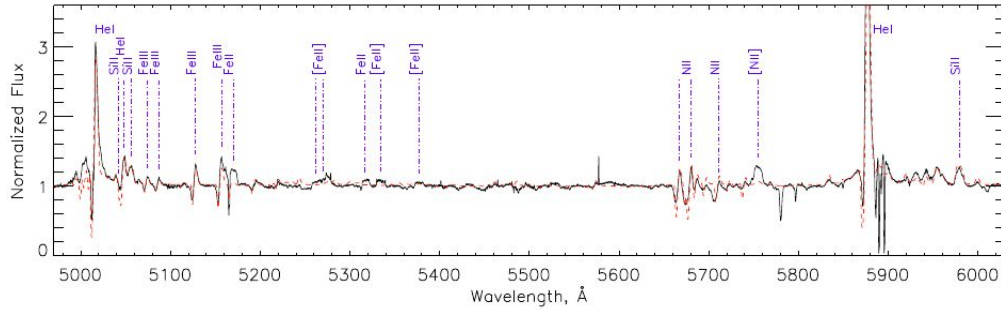


CMFGEN and Evolutionary Codes

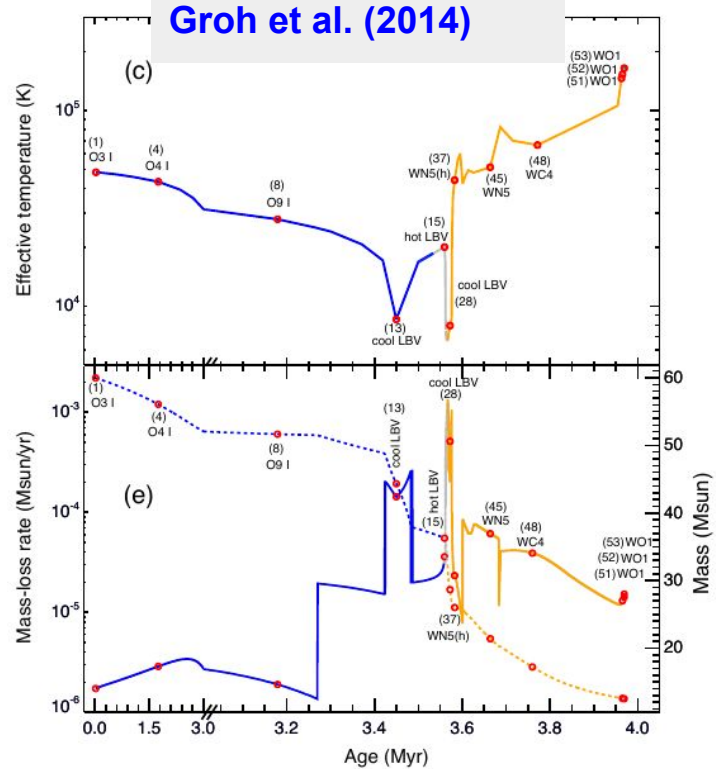
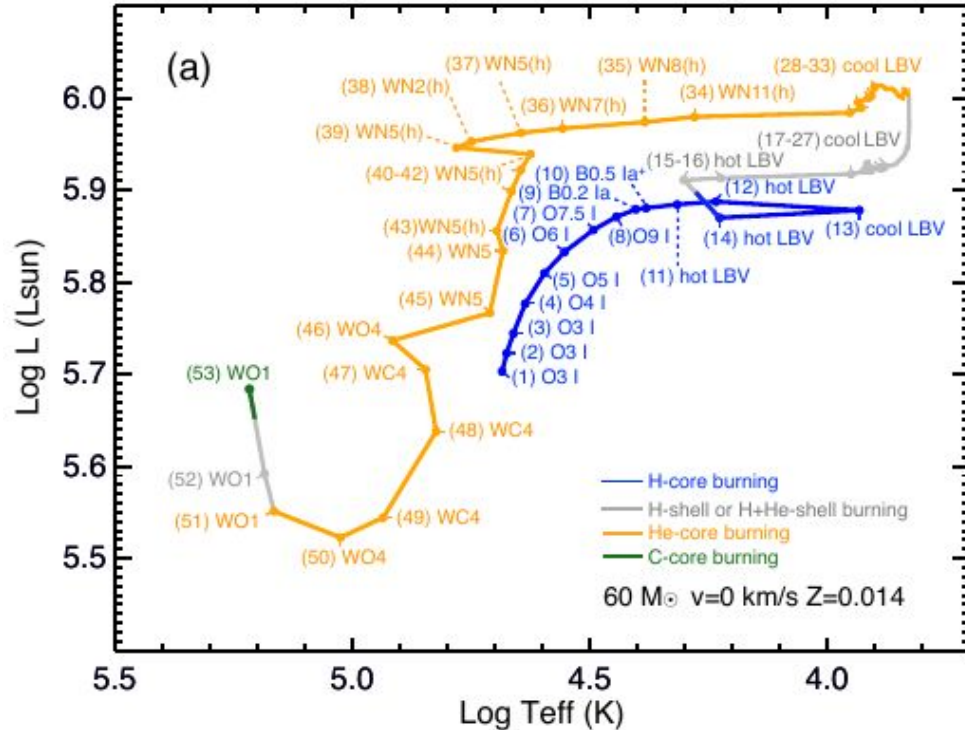


CMFGEN and Evolutionary Codes

Wray15-906

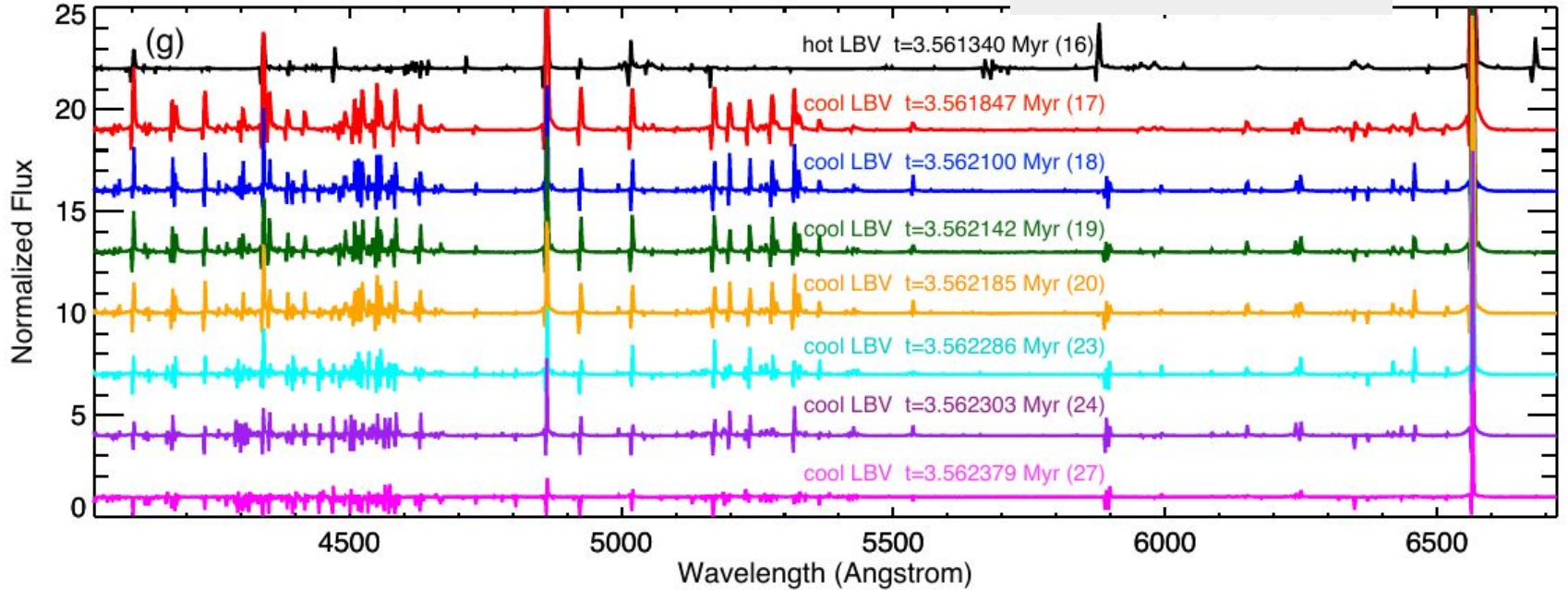


CMFGEN and Evolutionary Codes



CMFGEN and Evolutionary Codes

Groh et al. (2014)









CMFGEN: Grids of Models

Home All models WR models O models

CMFGEN models : 1408 models

<http://www.sao.ru/webmodels/models>

Filter ions: Al2 - AlIII - ArII - ArV - ArV - C2 - Cl - CIII - CIV - CaII - CaIV - CaSIX - CaV - Fe2 - FeII - FeIV - FeSEV - FeSIX - FeV - HI - He2 - HeI - Mg2 - N2 - NI - NIII - NIV - NV - Ne2 - NeIII - NeIV - O2 - OI - OIII - OIV - OSIX - OV - PIV - PV - S2 - SIII - SIV - SSIX - SV - Sk2 - SkIII - SkIV - All

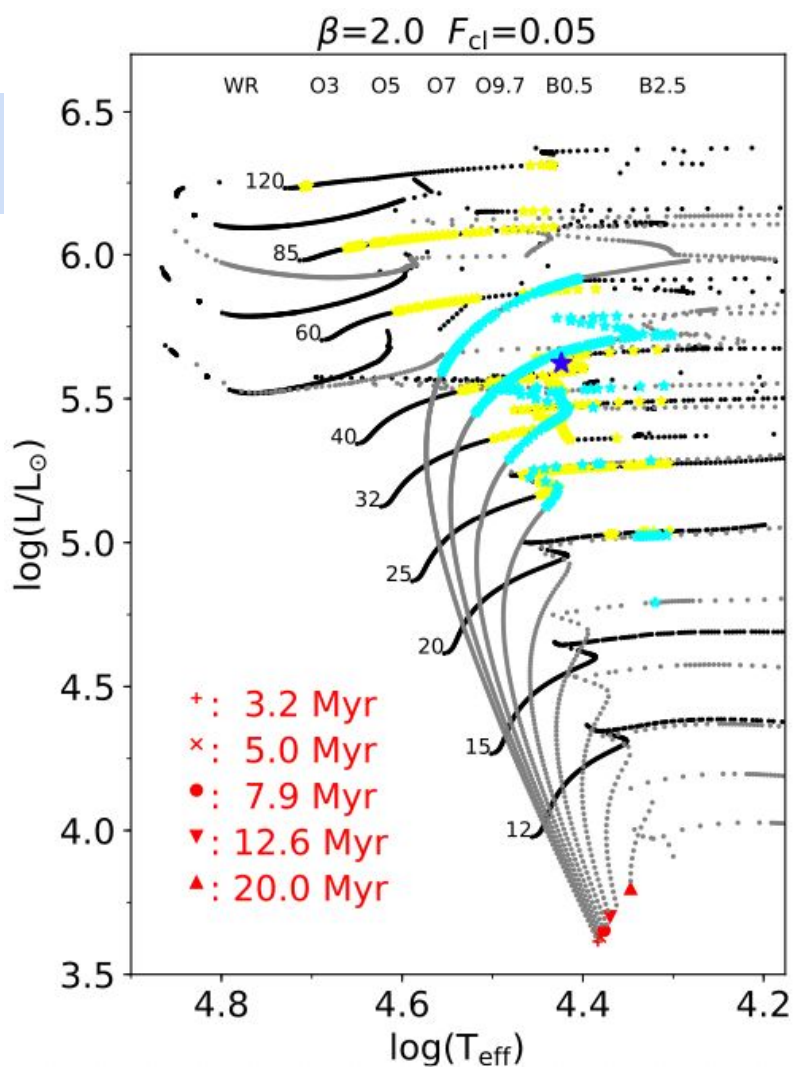
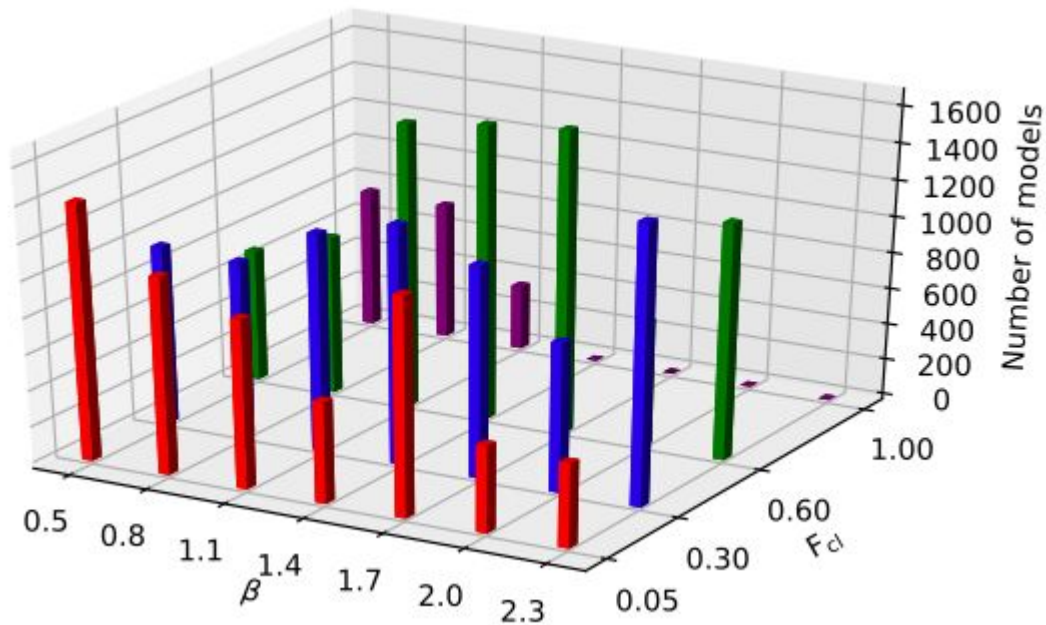
Name ▾	L / L_{sun} ▾	M_{dot} ▾	T_* ▾	T_{eff} ▾	Velocity Law ▾	V_{∞} ▾	CL_1 ▾	CL_2 ▾	Hydrogen ▾	C ▾	N ▾	O ▾	Fe ▾
 model1552	530000	1.8e-05	33000	30690	3: $\beta = 1.0$	300	0.1	100.0	1.9 / 31.8%	1.0e-04	3.0e-03	8.0e-04	4.9e-05 S N
 model1558	530000	2.8e-05	25000	23960	3: $\beta = 1.0$	300	0.1	100.0	1.9 / 31.8%	1.0e-04	3.0e-03	8.0e-04	4.9e-05 S N
 model1559	530000	3.3e-05	25000	23360	3: $\beta = 1.0$	300	0.1	100.0	1.9 / 31.8%	1.0e-04	3.0e-03	8.0e-04	4.9e-05 S N
 model1560	530000	2.8e-05	25000	23810	3: $\beta = 1.0$	270	0.1	100.0	1.9 / 31.8%	1.0e-04	3.0e-03	8.0e-04	4.9e-05 S N
 model1561	530000	2.8e-05	25000	23640	3: $\beta = 1.0$	250	0.1	100.0	1.9 / 31.8%	1.0e-04	3.0e-03	8.0e-04	4.9e-05 S N
 model1562	530000	2.8e-05	25000	23170	3: $\beta = 1.0$	220	0.1	100.0	1.9 / 31.8%	1.0e-04	3.0e-03	8.0e-04	4.9e-05 S N
 model1563	530000	2.8e-05	25000	22700	3: $\beta = 1.0$	200	0.1	100.0	1.9 / 31.8%	1.0e-04	3.0e-03	8.0e-04	4.9e-05 S N
 model1564	530000	2.8e-05	25000	21790	3: $\beta = 1.0$	170	0.1	100.0	1.9 / 31.8%	1.0e-04	3.0e-03	8.0e-04	4.9e-05 S N
 model1565	530000	1.8e-05	27000	26220	3: $\beta = 1.0$	300	0.2	100.0	1.9 / 31.8%	1.0e-04	3.0e-03	8.0e-04	4.9e-05 S N
 model1566	530000	1.8e-05	27000	26230	3: $\beta = 1.0$	300	0.3	100.0	1.9 / 31.8%	1.0e-04	3.0e-03	8.0e-04	4.9e-05 S N
 model1572	530000	3.5e-05	27000	24120	3: $\beta = 1.0$	300	0.5	100.0	1.9 / 31.8%	1.0e-04	3.0e-03	8.0e-04	4.9e-05 S N
 model1573	530000	3.5e-05	29040	23380	3: $\beta = 1.0$	250	0.5	100.0	1.9 / 31.8%	1.0e-04	3.0e-03	8.0e-04	4.9e-05 S N
 model1575	530000	3.5e-05	31000	21280	3: $\beta = 1.0$	180	0.5	100.0	1.9 / 31.8%	1.0e-04	3.0e-03	8.0e-04	4.9e-05 S N
 model1577	530000	2.9e-05	31000	23850	3: $\beta = 1.0$	200	0.5	100.0	1.9 / 31.8%	1.0e-04	3.0e-03	8.0e-04	4.9e-05 S N
 model1579	530000	3e-05	29040	23220	3: $\beta = 1.0$	200	0.5	100.0	1.9 / 31.8%	1.0e-04	3.0e-03	8.0e-04	4.9e-05 S N

CMFGEN: Grids of Models

Zsargo et al. 2020 *“Creating and using large grids of precalculated model atmospheres for a rapid analysis of stellar spectra”*

Mega grid of ~80 000 stellar atmospheric models is calculated. These models cover the region of the H-R diagram that is populated by OB main-sequence and WR stars with masses of 9-120 Msun. The grid provides UV, visual, and IR spectra for each model. Zsargo et al. 2020 used the surface temperature (T_{eff}) and luminosity (L^*) values that correspond to the evolutionary traces and isochrones of Ekström et al. (2012). Furthermore, they used seven values of β , four values of the clumping factor, and two different metallicities and terminal velocities.

CMFGEN: Grids of Models



CMFGEN: From Macrocosm to Microcosm

Processes

- 1) Bound-bound processes (line transitions)
- 2) Bound-free (photoionization/recombination)
- 3) Free-free (bremsstrahlung)
- 4) Low-temperature dielectronic recombination (LTDR)
- 5) Gamma ray transport/degradation
- 6) Auger ionization
- 7) Two photon emission
- 8) Electron scattering
- 9) Rayleigh scattering
- 10) Charge exchange
- 11) Collisional process
 - I **changing** collisions, excitation/deexcitation
 - Ionization/recombination

CMFGEN: From Macrocsm to Microcosm

Processes

12) Line broadening

Stark (linear, quadratic, van-der Waals) -- Electrons, protons, H, H⁻, He

Hyperfine structure, isotopic effects

13) Penning ionization

He I(1s 2s 3S) + H(1s) ---> HeI(1s2 1S) + H⁺ + e⁻

H(2s) + H(2s) → H(1s) + H⁺ + e⁻

14) Plasma effects (level dissolution)

15) Non-thermal ionization/excitation

16) High-temperature dielectronic recombination (HTDR)

17) Thermalization of electrons

18) Zeeman splitting

19) Raman scattering (symbiotic stars)

20) Molecules (B[e] stars, SNe, WC stars)

Above + chemical reactions

CMFGEN: Comparison with other codes

Puls, 2008

Table 1. Basic features and domains of applications of present state-of-the-art, NLTE, line-blanketed model atmosphere codes. Responsible authors in brackets.

	Detail/surf. (Butler)	TLUSTY (Hubeny)	CMFGEN (Hillier)	WM-basic (Pauldrach)	FASTWIND (Puls)	POWR (Hamann)	PHOENIX (Hauschildt)
geometry	plane-parallel	plane-parallel	spherical	spherical	spherical	spherical	spherical/ pl.-parallel
blanketing	LTE	yes	yes	yes	approx.	yes	yes
line transfer	observer's frame	observer's frame	comoving frame (CMF)	Sobolev	CMF	CMF	CMF/ obs.frame
temperature structure	radiative equilibrium	radiative equilibrium	radiative equilibrium	e ⁻ thermal balance	e ⁻ thermal balance	radiative equilibrium	radiative equilibrium
photosphere	yes	yes	from TLUSTY	approx.	yes	yes	yes
diagnostic range	no limitations	no limitations	no limitations	UV	optical/IR	no limitations	no limitations
major application	hot stars with negl. winds	hot stars with negl. winds	OB(A)-stars, WRs, SNe	hot stars w. dense winds, ion. fluxes, SNe	OB-stars, early A-sgs	WRs	stars below 10 kK, SNe
comments	no wind	no wind	start model required	no clumping	explicit/backgr. elements		molecules included, no clump.
execution time	few minutes	hours	hours	1 to 2 h	few min. to 0.5 h	hours	hours

CMFGEN: Comparison with other codes

There is, in general, very good agreement between the physical properties of massive O stars derived by modeling the same data both by FASTWIND and CMFGEN. There is no significant difference in the mean or median effective temperature found, although there is quite a bit of scatter. More interesting, perhaps, is the systematic 0.1 dex difference in the log g 's obtained by our fits using the two programs, with fastwind producing a lower surface gravity. We demonstrate that this 0.1 dex difference is quite significant to the mass discrepancy problem. The CMFGEN spectroscopic masses are in better agreement with the evolutionary masses, while fastwind's spectroscopic masses tend to be too low, consistent with the long-standing mass discrepancy.

Massey et al. 2013

CMFGEN: Comparison with other codes

X-Shooting ULLYSES: Massive Stars at low metallicity

IV. Spectral analysis methods and exemplary results[★]

A. A. C. Sander¹, J.-C. Bouret², M. Bernini-Peron¹, F. Backs³, J. M. Bestenlehner⁴, S. A. Brands³, P. A. Crowther⁴,
V. M. A. Gómez-González⁵, W.-R. Hamann⁵, A. Herrero^{6,7}, D. J. Hillier¹⁴, R. Kuiper¹⁵, C. J. K. Larkin^{1,8}, R. R.
Lefever¹, F. Martins⁹, O. Maryeva¹⁰, F. Najarro¹¹, L. M. Oskinova⁵, D. Pauli⁵, J. Puls¹², V. Ramachandran¹, E. C.
Schösser¹, H. Todt⁵, and J. S. Vink¹³

Useful References

"The Treatment of Non-LTE Line Blanketing in Spherically Expanding Outflows", Hillier & Miller, 1998

[The Treatment of Non-LTE Line Blanketing in Spherically Expanding Outflows - NASA/ADS](#)

"Constraints on the Evolution of Massive Stars through Spectral Analysis. I. The WC5 Star HD 165763", Hillier & Miller, 1998

[Constraints on the Evolution of Massive Stars through Spectral Analysis. I. The WC5 Star HD 165763 - NASA/ADS](#)

"Modeling the wind and photosphere of massive stars with the radiative transfer code CMFGEN", Groh, 2011

[Modeling the wind and photosphere of massive stars with the radiative transfer code CMFGEN - NASA/ADS](#)

WR (works by Crowther); OB stars (works by Martins; Bouret, Marcolino); LBVs (works by Groh; Najarro); SN (works by Dessart); IR range (works by Najarro)

Thank you for your attention!

Four horizontal lines of varying colors (magenta, lime green, blue, and teal) are positioned below the text, extending across the width of the slide.